Peer-reviewed version available at *Quaternary* **2019**, *2*, 4; doi:10.3390/quat2010004

Review

A window into Africa's past hydroclimates: the SISAL_V1 database contribution

Kerstin Braun [1,2,*], Carole Nehme [3,4], Robyn Pickering [5,6], Mike Rogerson [7] and Nick Scroxton [8,9]

[1] Institute of Human Origins, School of Human Evolution and Social Change, Arizona State University; kbraun2@asu.edu
[2] African Centre for Coastal Paleoscience, Nelson Mandela University, Port Elizabeth, South Africa
[3] Department of Geography, IDEES 6266 CNRS, University of Rouen-Normandy, Mont Saint-Aignan, France; carole.nehme@univ-rouen.fr
[4] Analytical, Environmental & Geo-Chemistry, Department of Chemistry, Vrije Universiteit Brussel, Belgium
[5] Department of Geological Sciences, University of Cape Town, Cape Town, South Africa; robyn.pickering@uct.ac.za
[6] Human Evolution Research Institute, University of Cape Town, Cape Town, South Africa
[7] School of Environmental Sciences, University of Hull, Hull, UK; M.Rogerson@hull.ac.uk
[8] University of Massachusetts Amherst, Amherst, MA, USA; nscroxton@umass.edu
[9] Massachusetts Institute of Technology, Cambridge, MA, USA

* Correspondence: kbraun2@asu.edu; Tel.: +1 480 965 1077; *All authors contributed equally and are listed alphabetically*

Abstract: Africa spans the hemispheres from temperate region to temperate region, has a long history of hominin evolution and yet has a relatively poorly understood Quaternary climate history. Speleothems, as archives of terrestrial hydroclimate variability, can help reveal this history, and here we review the progress made to date, with a focus on the first version of the Speleothem Isotopes Synthesis & Analysis (SISAL) database. The geology of Africa has limited development of large karst regions to four areas - the northern and eastern coasts bordering the Mediterranean and the Indian Ocean, west Africa and southern Africa. Exploitation of the speleothem palaeoclimate archives in these regions is uneven, with long histories of research in South Africa and Morocco but no investigations elsewhere e.g. West Africa. Consequently, the evidence of past climate change reviewed here is irregularly sampled in both time and space. Nevertheless, we show evidence of migration of the monsoon belt, with enhanced rainfall during interglacials observed in northeast Africa, southern Arabia and the northern part of southern Africa. Evidence from East Africa indicates significant decadal and centennial scale rainfall variability. In northwestern and southern Africa precession and eccentricity influence speleothem growth, largely through changing synoptic storm activity.

Keywords: speleothem; hydroclimate; monsoon; ITCZ; SISAL; oxygen isotopes

1. Introduction

Speleothems are secondary cave carbonates and provide valuable archives of past hydroclimates. In this study, we focus on the speleothem record from Africa, using the SISAL_v1 database [1, 2] as a starting point. We include southern Arabia and Madagascar as part of the African region. Africa covers an area of over 30 million km^2 and makes up 20% of the earth's land surface. It is also the only continent to stretch from the northern temperate to the southern temperate zones, which should theoretically allow an exploration of latitudinal migrations of climatic belts. However, the density of speleothem records is much smaller than in other regions. The paucity of records is partly due to the underlying bedrock geology [3], which is dominated by PreCambrian basement rocks, with little outcrop of carbonates or evaporites (Figure 1), [4]. Africa is also the hottest continent on earth, with

60% of the entire land surface consisting of drylands and deserts [5], which reduces the potential for formation and preservation of speleothem records.

Africa has a long history of speleothem research, with some of the earliest speleothem studies conducted in South Africa [6, 7]. These early days of research remained focused on the South African record but from the early 2000s onwards, speleothem studies come from across the continent (Figure 1). While some of the early records were dated using radiocarbon [7], the majority of records are dated with uranium-thorium. The advent of uranium-lead dating of speleothems [8] saw the direct dating of the early hominin cave sites in South Africa [9, 10, 11] and while these deposits have great potential as archives of past hydroclimates [12, 13] they are virtually untapped.

In this paper we use the SISAL_v1 database (Figure 1) as a starting point to explore the speleothem record of Africa, southern Arabia and Madagascar, focusing on regional trends, connections between the regions, and changes in hydroclimate. We present an overview of the 59 speleothem records from the region, of which 19 are in SISAL_v1 (Table 1). We assess their key findings, provide regional syntheses of the results, and outline some key research questions that should frame future research.

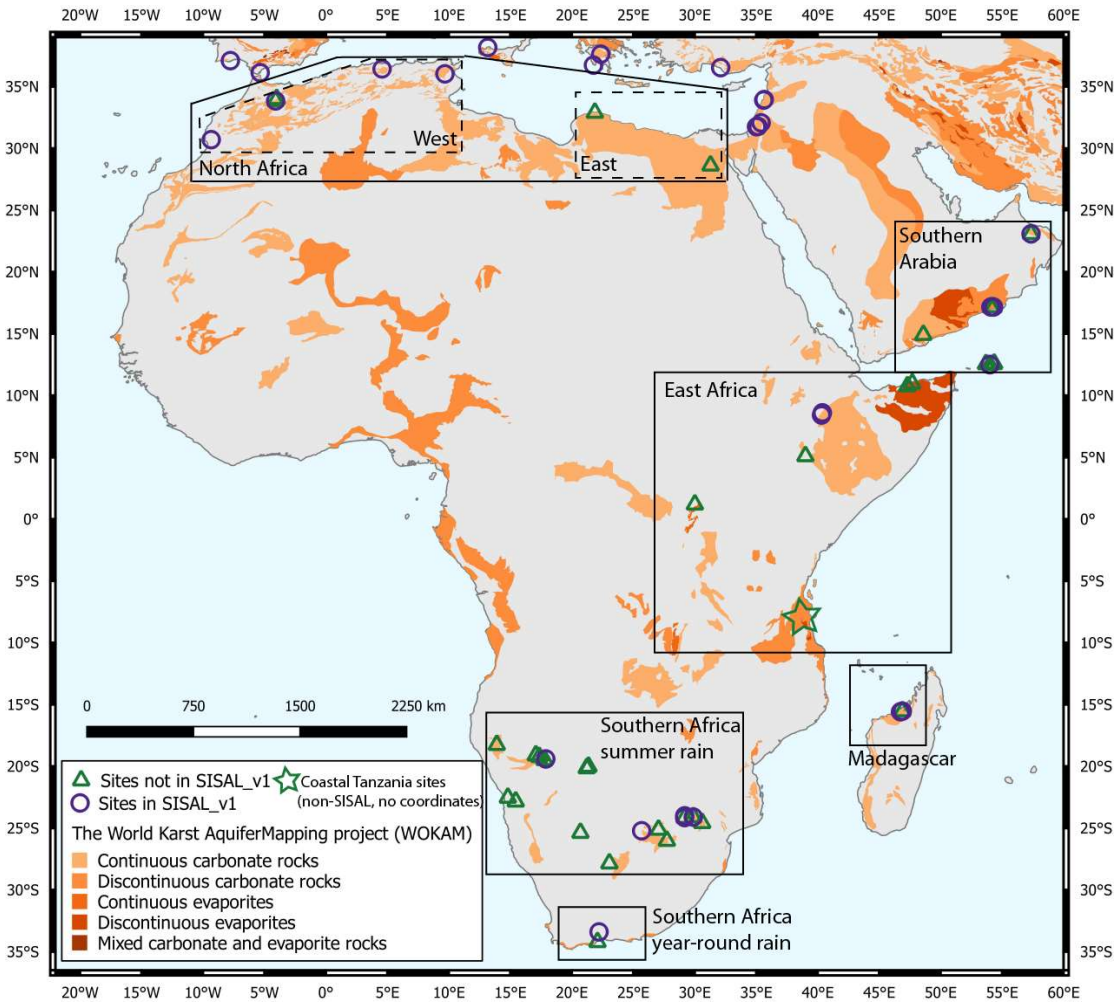

Figure 1. A map of Africa, including Madagascar and southern Arabia highlighting the distribution of karst regions through the mapping of carbonates and evaporites (data provided by The World Karts Aquifer Mapping Project, WOKAM, 4) and the locations of speleothem records (open circles represent those included in SISAl v1; triangles represent sites not included in SISAL v1).

Table 1. List of speleothem records from the Africa region. Column headings in italics represent field names that can be searched in the SISAL database. Entities without a SISAL entity_id are not included in the database. Minimum and maximum years refer to minimum and maximum ages of the stable isotopic records (which may be extrapolated from measured ages); Minimum and maximum ages in italics are measured values in records where age models for proxies were not easily accessible, asterisks mark minimum and maximum ages at sites where speleothem dating was used in presence/absence studies or to date archaeological deposits - these records often have no proxy records or no continuous age models if proxies were analyzed.

site_name	*stie_id*	**Country**	*latitude* **(N)**	*longitude (E)*	*elevation (m amsl)*	*entity_name*	*entity_id*	**Min. year (BP)**	**Max. year (BP)**	**Reference**
Achere Cave	114	Ethiopia	8.60	40.37	1534	Ach-1	229	4523	4968	[64]
Aigamas		Namibia	-19.11	17.07				*112000**	*129900**	[96]
Aikab		Namibia	-19.11	17.07				*7500**	*10600**	[96]
Anjohibe Cave	94	Madagascar	-15.53	46.88	131	AB3	187	-64	1673	[77]
						AB2	188	-64	1343	[73]
						MA3	189	650	1580	[78]
						ANJB-2	190	141	9027	[81]
						MA1		*-45*	*3412*	[72]
						MA2		*-45*	*7340*	[72]
Anjokipoty Cave	32	Madagascar	-15.58	46.73	~40	MAJ-5	107	183	9880	[123]
Bero Cave	33	Ethiopia	8.42	40.31	1363	Bero-1	108	-55	7750	[65]
Bone Cave		Botswana	-20.14	21.21	1000	BC97-14		-47	273	[124]
Buffalo Cave	148	South Africa	-24.14	29.18	1140	Boffalo Cave Flowstone	323	1,517,550	1,989,850	[12,13]
Cango Cave	74	South Africa	-33.39	22.21	~700	V3	163	41	47978	[6, 125, 100]
Casecas Cave		Yemen	12.56	54.31	542	STM5		*12*	*856*	[62]
Cold Air Cave	7	South Africa	-24	29.18	1420	T5	45	466	4379	[126]
						T7_1999	46	-46	2506	[127, 128]
						T7_2001	47	-46	6406	[98]
						T8	48	-48	24380	[85]
						T7_2013	49	-46	314	[99]
Crevice Cave		South Africa	-34.21	22.09	15	composite record		53060	90500	[101]

Dante Cave	99	Namibia	-19.4	17.88		DP1_2013	197	18	4618	[87]
						DP1_2016	198	11	487	[82]
Defore Cave	170	Oman	17.17	54.08	150	S3	366	-46	731	[55]
						S4		*9020*	*10864*	[63]
Dimarshim Cave		Yemen	12.55	53.68	350	D1		-50	4400	[63]
Dragons - breath		Namibia	-19.48	17.79					*8,800**	[96]
Drotsky's Cave (Gcwihaba Caves)		Botswana	-20.02	21.36				*750**	*41900**	[129,130]
						Stalagmite 1		*14125**	*16190**	[131]
						Stalagmite 2		*3663**	*5860**	[131]
						Stalagmite 3		*1185**	*5375**	[131]
						1.0m core		*197400**		[40]
						0.5m core		*5360**	*14520**	[40]
Echo Cave		South Africa	-24.58	30.61	1030			*2675**	*231900**	[95, 96]
Gaalweyte Cave		Somalia	10.98	47.69				*5000**	*75500**	[96]
Gladysvale Cave		South Africa	-25.12	27.05				*7450**	*571380**	[90]
Grotte de Piste	135	Morocco	33.84	-4.09	1260	GP2	285	2537	11416	[49]
Grotte Prison de Chien		Morocco	34	-4	360	HK1		*18870*	*36470*	[46]
						HK3		*4240*	*27480*	[46]
Gueldaman Cave	81	Algeria	36.43	4.57	507	stm2	173	4039	6191	[16]
						stm4	174	3193	5793	[16]
Guinas Meer		Namibia	-19.23	17.35				*13500**	*61400**	[96]
Harasib		Namibia	-19.48	17.79				8500*	107600*	[96]
Hayla Cave		South Africa	10.76	47.30	1800			*4000**	*260400**	[40, 96]
Hoq Cave		Yemen	12.59	54.35	335	STM1		*-17*	*5717*	[62]
						STM6		*777*	*4608*	[62]
						Hq1		*146*	*7708*	[62]
Hoti Cave	152	Oman	23.08	57.35	800	H5	327	6026	9607	[53]

						H5		*6220*	*10760*	[52, 51, 63]
						H12		*230*	*6341*	[52, 63]
						Flowstone		*82000*	*125700*	[50] [52]
						H4		*112900*	*121600*	[50] [52]
						H1		*77620*	*82460*	[52]
						H10		*8250*	*10150*	[52]
						H11		*8130*	*9060*	[52]
						H13		*124000*	*387000*	[52]
						H14		*6410*	*8470*	[52]
Ifoulki Cave	42	Morocco	30.71	-9.33	1250	IFK1	188	-3	1160	[47]
Kiomoni Quarry Cave		Tanzania						*17430**	*19270**	[71]
La Mine Cave	83	Tunisia	36.03	9.68	975	Min-stm1	176	5366	23168	[44]
Lobatse Cave	30	Botswana	-25.21	25.68	1200	LII4	103	21425	27206	[91, 92]
						LII4-KH	104	21458	50943	[91, 92]
Mafuriko Quarry		Tanzania	5.10	39.00				*28100**	*39400**	[132, 71]
Makapan Cave		South Africa	-24.16	29.18				*202000**	*324000**	[133]
Mampombo Cave		Tanzania						*31560**	*104640**	[71]
Matupi Cave		Democratic Republic of Congo	1.19	30.01	1100	MAT 23		*13260**	*14820**	[40]
						MAT16			*"modern"*	[40]
						MAT11		*40100**		[40]
						MAT13		*990**	*50330**	[40]
Moomi Cave	138	Yemen	12.5	54	400	M1-5	293	11086	27370	[59]
						M1-2		40379	53484	[58]
Mukalla Cave		Yemen	14.92	48.59	1500	Y99		*119141*	*358887*	[54]
						Y97-4		*5630*	*185600*	[54]
						Y97-5		*8790*	*233300*	[54]
Namaingo Cave		Tanzania						*560**	*2640**	[71]

Nangoma - Nakitara Cave		Tanzania						*53560**	*77150**	[71]
Orumana Cave		Namibia	-18.26	13.89	1450	Orum-1		*986*	*47301*	[86]
PP29		South Africa	-34.21	22.09	10	46745		67600	112400	[39]
						46746a		82700	99500	[39]
						46746b		75000	98800	[39]
						46747		41500	61300	[39]
						138862.1		58500	89200	[39]
						138862.2a		102900	109900	[39]
						138862.2b		82920	88000	[39]
						142828		51000	108400	[39]
Qunf Cave	159	Oman	17.17	54.3	650	Q5	351	308	10558	[63]
						Q5		*400*	*10470*	[56]
						Q11		*3738*	*4929*	[56]
Rössing Cave		Namibia	-22.53	14.80	332			*26530**	*480000**	[121, 134]
						KOO933		*117000**	*413000**	[121];
						KOO931		*363000**	*480000**	[121, 134]
						KOO930		*89000**	*480000**	[121, 134]
						KOO929		*369000**	*439000**	[121, 134]
Rukiessa Cave	22	Ethiopia	8.60	40.38	1618	Merc-1	87	-53	56	[67, 68]
						Asfa-3	88	-53	52	[67, 68]
Staircase Cave		South Africa	-34.21	22.09		46322		202400	279100	[39]
						46330a		210800	215800	[39]
						46330b		173500	205700	[39]
						46861		172000	283200	[39]
						50100		194500	247800	[39]
						142819		129900	334700	[39]
						142820		160900	335600	[39]
Sterkfontein Cave		South Africa	-26.02	27.73	1450			*10000**	*200000**	[96]
Sudwala Cave		South Africa	-25.37	30.7	975	SC1		*12790*	*40220*	[93]
								*1160**	*403290**	[93]

Preprints (www.preprints.org) | NOT PEER-REVIEWED | Posted: 1 October 2018 doi:10.20944/preprints201810.0016.v1

Peer-reviewed version available at Quaternary 2019, 2, 4; doi:10.3390/quat2010004

Susah Cave		Libya	32.89	21.87	200	SC-06-01		31945	66636	[15]
						SC-06-01 parallel		30755	34850	[15]
Tinkas Cave		Namibia	-22.84	15.44	425			*224000**	*337000**	[134]
Wadi Sannur Cave		Egypt	28.62	31.28	200	WSS		*136460*	*188120*	[43]
						WS-5d		*127923*	*365921*	[17]
Wolkberg Cave	172	South Africa	-24.1	29.88	1450	W5	377	39742	57872	[89]
								*1,520**	*29,560**	[7]
Wonderwerk Cave		South Africa	-27.85	23.06	1680	W-1		*900*	*34800*	[94]

2. Key climate drivers across Africa

African climate systems are mostly arranged in zonal patterns with variable seasonal rainfall. The northern and southern extremes of the continent experience Mediterranean climates with dry summers and winter rains due to the equatorward displacement of the westerlies. Towards the equator, the Sahara and Namib-Kalahari deserts in the north and south respectively, are dominated by year-round subtropical anticyclones. Tropical climates between the two desert belts are dominated by the seasonal migration of the Intertropical Convergence Zone (ITCZ) that leads to a bimodal seasonal rainfall distribution in equatorial regions and a single rainfall season in the more distal regions, closer to the desert belts. This overall pattern is regionally modified by zonal circulation and topography; major drivers and patterns are summarized here for the regions from which speleothem records are available (Figure 1).

The northwestern part of the Mediterranean climate region of Northern Africa (northwest of the Atlas Mountains) receives rainfall from Atlantic Ocean westerly storms that are generally associated with baroclinic activity over the North Atlantic or the North Atlantic Oscillation - NAO [14]. Semi-arid and arid climates dominate much of northern Africa east of the Atlas Mountains and most cave sites in this region are currently dry with no active speleothem deposition [15, 16, 17]. Low amounts of winter rainfall along the northern coasts of Africa are usually brought by localized Mediterranean cyclones rather than from the Atlantic Ocean [14]. Long-term climatic variability across much of Northern Africa is dominated by alternation between arid and pluvial periods, which arise from a combination of intensified winter rainfall, analogous to the modern climatology influenced by the NAO synoptic system driving cyclones in the Western and central Mediterranean and northward migration of the monsoon belt. The latter changes are well known from a range of marine and terrestrial archives and occur during phases of high northern hemisphere summer insolation [18, 19, 20, 21, 22, 23, 24].

Preprints (www.preprints.org) | NOT PEER-REVIEWED | Posted: 1 October 2018 doi:10.20944/preprints201810.0016.v1

Peer-reviewed version available at *Quaternary* **2019**, *2*, 4; doi:10.3390/quat2010004

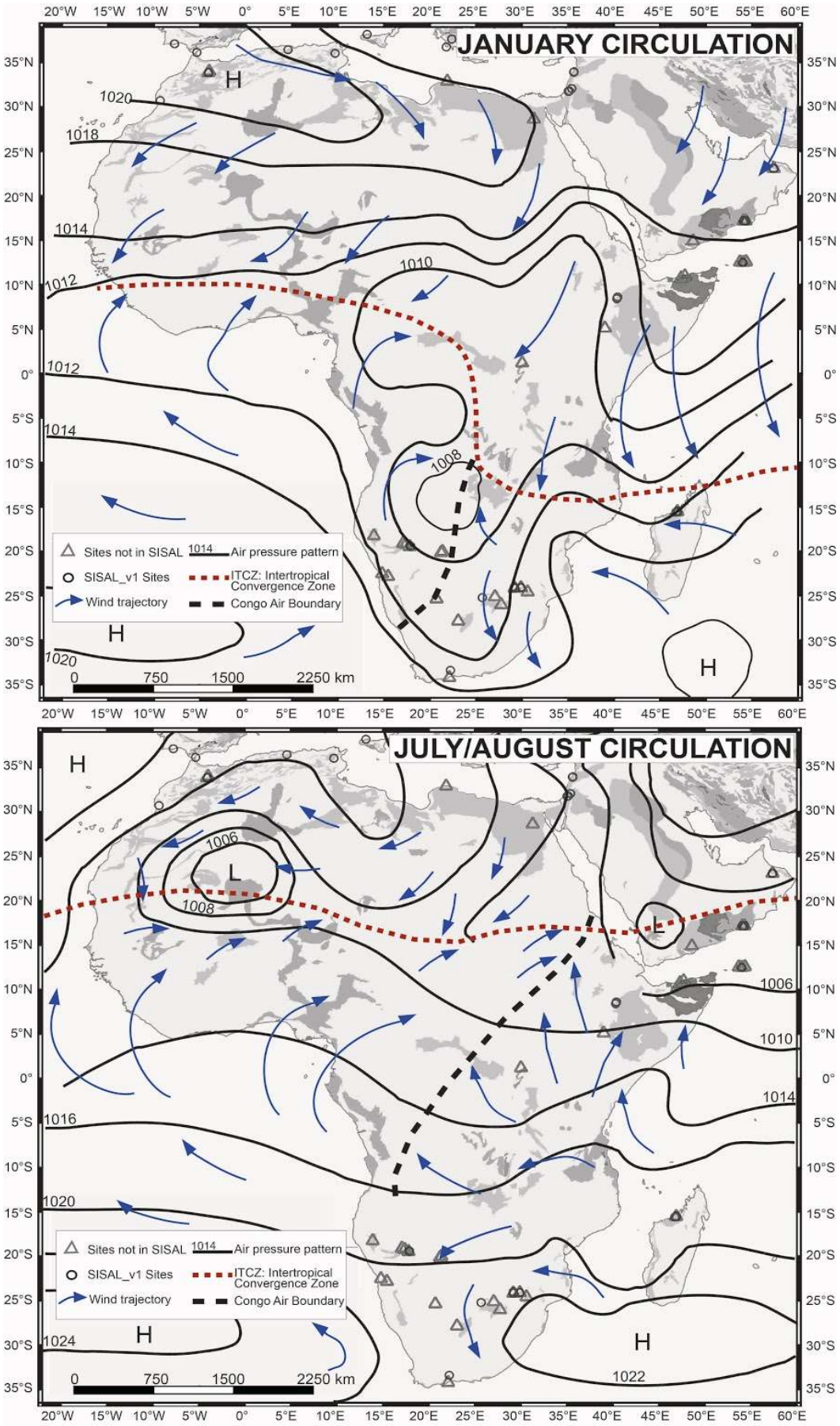

Figure 2. Regional climate and circulation patterns. Adapted from Gasse, 2000 and Nicholson, 1996, including locations of speleothem records (open circles represent those included in SISALv1; triangles represent sites not included in SISAL v1): (**a**) January (**b**) July/August.

In eastern Africa, southern Arabia and Madagascar, the meridional passage of the ITCZ over the year controls rainfall seasonality. Summer monsoonal climates occur at higher latitudes of either hemisphere, while double wet seasons in the spring and autumn occur at lower latitudes where there are two overhead passes of the ITCZ each year [25]. Rainfall over these regions shares a common moisture source: the western Indian Ocean [26] Indian Ocean SSTs are known to play a strong role in modulating modern rainfall amount [26, 27, 28, 29] via changes in Walker Circulation. A warming of the western Indian Ocean sea surface temperatures (SSTs) and cooling of Eastern Indian Ocean weakens the longitudinal SST gradient and leads to stronger westerly winds. This results in a shift in the locus of rainfall towards East Africa – a positive Indian Ocean Dipole event [30, 31]. Climate variability on decadal to millennial timescales is dominated by similar but lower frequency "Indian Ocean Dipole-like" modes [32, 33, 34]. On orbital timescales, the relationship between Indian Ocean SST and rainfall in Eastern Africa switches sign as low glacial SST coincide with low sea levels and the exposure of the Sunda Shelf which rearranges the Walker circulation to cause an increase of rainfall [24].

Located at the southernmost extent of the seasonal ITCZ migration, the subtropical summer rainfall regions of Southern Africa are affected by similar drivers as Eastern Africa. Under present day conditions, the positive phase of the Indian Ocean Dipole leads to increased rainfall in the eastern part of this region [35]. In the western parts, in northern Namibia and Botswana, the location of the Inter-Ocean Convergence Zone (IOCZ; also known as Congo Air Boundary), a western branch of the ITCZ, determines rainfall amounts and shifts of the moisture source between the tropical Atlantic and western Indian Ocean [36]. Past climate changes in the eastern parts of the southern African summer rainfall region also follow similar patterns as East Africa, with Indian Ocean SST being and important driver during interglacials, but the influence of sea level changes taking over on glacial-interglacial timescales [24]. In the western parts of the southern African tropics, the tropical rain belt appears to have expanded and contracted between interglacial and glacial phases [37]. The year-round rainfall region on the south coast of Africa gets rainfall from complex interactions of tropical and temperate atmospheric systems [38] that vary in their intensities on glacial-interglacial timescales related to the positions and strengths of the westerlies, subtropical anticyclones, and continental summer heat low [39].

The ultimate goal of the SISAL initiative is to look at how climatic systems may have operated in the past, as indicated by the speleothem records. As many of the karst regions in Africa are located in semi-arid zones there has been a tendency in the literature to assume that the growth phases of speleothems at particular sites are indicative of wetter conditions, with hiatus corresponding to drier conditions [17, 15, 40]. However, there are multiple reasons why stalagmites can stop growing that are unrelated to climate, notably changes in drip hydrology [41]. Therefore, we argue that the interpretation of single speleothem growth phases as definitive wet/dry indicators should be avoided. Instead, we advocate for a combined approach, where replicating growth phases, corroboration by independent proxies or repeated correlation with climate drivers are used to provide support for speleothem growth phases as proxies of past climates.

3. Distribution of speleothem isotopic records in space and time

3.1. North Africa: Eqypt, Libya, Tunisia, Algeria, Morocco

Much of North Africa comprises sediments deposited in the Tethys basin, which have been uplifted during the Alpine-Atlasic Orogeny [42]. Consequently, it is richer in carbonate sediments than most regions on the continent and has strong potential for speleothem-based palaeoclimatology (Figure 1).

In Egypt, one stalactite from Wadi Sannur Cave [43] has provided a record indicating six wet phases between ~188 ka and 136 ka. A stalagmite with double growth axes (WS-5d) from the same cave shows three wet phases at 335 ± 12 ka, ~219.4, ± 7.3 ka and 129.1 ± 1 ka, corresponding to MIS 9, 7c and 5e, [17], but age reversals within the 18 dating analyses do not allow the construction of a reliable age model. The absolute $\delta^{18}O$ values of the speleothem are ~5‰ lower than speleothems considered to reflect a Mediterranean moisture source. Consequently, they are, interpreted as reflecting a long transport distance for atmospheric vapor [17], and suggest the primary driving mechanism is northward migration of the African monsoon system.

Further west, a single speleothem record has been published from Susah Cave in Libya [15], with three main humid periods during MIS3 dating to 65–61 ka, 52.5–50.5 ka and 37.5–33 ka. The first and third phase occur during times when orbital precession causes relatively increased summer insolation on the northern hemisphere. The second growth period represents the first evidence for high obliquity leading to pluvial conditions in the North African subtropics in the same manner as precession [15]. In between the three main deposition phases short periods of growth show a marked temporal coherence with Greenland Dansgaard-Oeschger interstadials [15]. Variations of speleothem $\delta^{18}O$ are in phase with changes of Greenland ice core $\delta^{18}O$, supporting a distal moisture source from the Atlantic Ocean, likely supplied by winter cyclones. Values of $\delta^{18}O$ also are disconnected from growth rate changes, which suggests that rainfall amount and rainfall source at Susah Cave change independently.

Tunisia is equally poorly represented, providing only one, short speleothem record from La Mine Cave that grew between 20 and 5 ka [44]. Oxygen isotopes show a two-step change from the late glacial into the Holocene, which may reflect freshening of the Mediterranean as sea levels rose [45], varying origin of source waters [15] or changes in precipitation amount. Carbon isotopes show a pronounced Bølling-Allerød/Younger Dryas oscillation, with the cool periods exhibiting wetter conditions [44]. The stalagmite ceased growth at 6 ka, possibly due to insufficient water availability [44].

Despite probably having the most outstanding karst of the western North African region, Algeria has provided only two speleothem records from Gueldaman Cave. These provide a decadal scale isotopic record from ~6.2 to ~3.3 ka [16]. The record and its archaeological context show three dry periods from 4.4 to 3.8 ka [16].

At least four caves have been extensively investigated in Morocco. Aufous cave southeast of the Atlas Mountains, Ifoulki Cave, Grotte Prison de Chien and Grotte de Piste to the northwest. Stalagmites from Aufous are beyond the range of U/Th dating, and so are at least 500 ka old. Grotte de Piste, Grotte Prison de Chien, and Ifoulki Cave have provided multiple stalagmite samples. Two speleothems from Grotte de Piste and Grotte Prison de Chien display prominent oscillations between calcite and aragonite, which reflect variations in climate with aragonite more common in drier conditions, and calcitic speleothems considered evidence of relatively humid conditions [46]. At Ifoulki cave, a stalagmite recording the last millennium (790 to 1953 CE) shows strong wet-dry variability at wavelengths of 15, 62 and 200 years [47], attributed to the NAO. The MCA (centered on 1120 CE) also exhibits evidence of a relatively dry climate, whereas the Little Ice Age phase, centered on ~1700 CE, is wet [48]. A similar influence of the NAO was also found for a Grotte de Piste speleothem during the mid-Holocene in which climatic oscillations were anti-correlated with European records. A positive correlation with the European records during the early Holocene suggests that changes in the ice volume on the northern hemisphere at the time lead to large scale reorganizations of oceanic and atmospheric circulation systems affecting the structure and "mode" of the NAO [49].

3.2. Eastern Africa, Arabia and Madagascar

3.2.1. Southern Arabian Peninsula

At the most northerly site in Arabia, Hoti Cave in northern Oman, speleothem growth is largely confined to interglacials: Marine Isotope Stages (MIS) 1, 5e, 5a, 7a, 9 and possibly 11 [50, 51, 52]. A positive excursion in $\delta^{18}O$ indicates the end of the early Holocene pluvial occurred at 6.1 ka [53]. MIS5e had more negative $\delta^{18}O$ than other interglacials, suggesting it was wetter [51]. Three speleothems from Mukalla Cave in southern Yemen replicate both the growth phase and $\delta^{18}O$ results from Hoti Cave, with additional growth at 5c and 7e, indicating that wet interglacials were a feature of the entire southern Arabian Peninsula [54]. Interglacial biased growth suggests that rainfall in Arabia responds more to the 100kyr glacial/interglacial cycles than to the 23kyr precession cycle variability observed in upwelling and wind strength proxies in the Arabian Sea [51], with important implications for Out of Africa routes of human migration [54].

Records from Qunf and Defore Caves in southern Oman provide a record of southern Arabian hydroclimate over the Holocene [55, 56; 57]. The end of the deglacial increase in moisture is abrupt at 9.6 ka again, almost synchronous with the NGRIP ice core record. There is a dry 8.2 ka event, and the end of the pluvial period is more gradual, between 6.5 and 4 ka, than the abrupt change at Hoti Cave to the north. $\delta^{18}O$ values during the last 1.5 ka are considerably more enriched (drier conditions) than the early and mid-Holocene [56]. An annually resolved record of the last 780 years shows significant centennial scale variability that may match variability in solar output [55], as does early Holocene variability at Hoti Cave [53]. During the last millennium wetter conditions are associated with the MCA and dryer conditions during the Little Ice Age, consistent with the previously established teleconnections of warm Northern Hemisphere to a wetter Arabian Peninsula [57]. However, drying conditions in the 20th century occurred despite Indian Ocean warming suggesting that modern climate change may be producing a different response in Arabian Peninsula hydroclimate to the warmer-wetter response in the paleoclimate record [55].

Further south, rainfall on the island of Socotra comes in two seasons from the double passage of the ITCZ. The Haggenher mountains act as moisture barriers such that caves in the south-west (Dimarshim) record the southwestern spring rains, while caves in the north-east (Hoq, Casecas, Moomi) record the northeasterly autumn rains. Speleothem $\delta^{18}O$ records from Moomi Cave show remarkable similarity to the NGRIP ice-core record during MIS 4 [58], and the deglaciation [59]. Warmer interstadials in Greenland such as the Dansgaard-Oeschger (D/O) events [60, 61] and the Bolling-Allerod coincide with wetter conditions in north-east Socotra, while stadials such as Heinrich events and Younger Dryas, coincide with drier conditions. The transitions during the climatic oscillations of the deglaciation are more gradual than the Greenland ice core response, comparable to other northern hemisphere monsoon records around the Indian Ocean.

There is a gradual decline in $\delta^{18}O$ in the eastern caves of Socotra (Hoq and Casecas Caves) between 6.0 and 3.8 ka [62], consistent with a gradual southerly shift of the ITCZ position over the course of the Holocene as a response to changing orbital forcing. During the late Holocene, anti-correlation occurs between the monsoonal records of Oman and the inter-monsoon records of Socotra, with a gradual wettening at Dimarshim cave over the last 4.4 ka [63]. Locally, this result was ascribed to changing wind paths to a more oceanic route as the south-west monsoon weakens. Regionally, this result is consistent with a southerly movement of the summer ITCZ over the course of the Holocene: the total amount of precipitation decreases at the northern fringes of the monsoon (Oman) but increases in areas closer to the equator (Socotra) [62, 63].

3.2.2. Mainland East Africa

Annually laminated stalagmites from the Mechara karst (notably the Achere-Aynage, Bero, Rukiessa and Goda Mea caves) in Ethiopia have provided short but high-resolution records of the mid-Holocene [64; 65] through to the last interglacial [66]. Recent growth over the twentieth century [67], and cave monitoring [68] provide a solid basis for interpretation of the records. While climatically the records are interpreted in terms of rainfall amount, the suggested mechanism may well be related to degassing and in-cave processes rather than a strict atmospheric control [64; 65]. The complex double wet season climate of the region, with relatively low variability in precipitation $\delta^{18}O$ compared to

differences arising from mixing within karst aquifers and possible in-cave fractionation effects makes simple wetter/drier climatic interpretations from the oxygen isotope proxy alone difficult. To overcome these complications, stalagmite records from this region typically rely on multi-proxy approaches, including morphology, fluorescence [64] biomarker analysis [69] and forward $\delta^{18}O$ modelling [65] to aid paleoclimate interpretations. Forward modelling suggests that decreases in $\delta^{18}O$ likely reflect increases in summer rains or decreases in spring rains.

Together these studies indicate persistent decadal-scale variability in all studied periods in Ethiopia, potentially related to ITCZ movement and western Indian Ocean SSTs. More negative $\delta^{18}O$ in the early Holocene likely results from long term orbital changes [65]. Mean $\delta^{18}O$ composition within growth phases from 129 to 108 ka (-3.82 to -7.77‰) were even lower than modern and Holocene stalagmites, indicative of wetter conditions [66].

Twelve speleothems from six caves were collected from three different areas spanning the eastern Tanzanian coast [70]. Most of these speleothems were either too porous or had too much detrital Th to produce reliable U-series dates, and even dateable samples had low U content, reducing dating precision [71]. However, the Mafuriko Quarry $\delta^{13}C$ record shows significant millennial-scale fluctuations between 39 and 27 ka. Although the age model prevents 1:1 association, the record appears to show wetter conditions during Dansgaard-Oeschger events 6-8.

3.2.3. Madagascar

Speleothems from two caves in the north-west of Madagascar (Anjohibe, Anjokipoty) provide insight into southern hemisphere monsoon dynamics. The first records from the region showed Walker circulation influences on hydroclimate over the past 500 years, with stalagmite layer width correlating with the Southern-Oscillation Index [72]. [73] produced a high-resolution isotope record covering the last 1700 years, showing in-phase coherence at the multi-decadal scale with the Oman speleothem record [55], and with lake-based hydroclimate reconstructions across East Africa at the multi-centennial scale [74, 75, 76]. These results suggest that sea surface temperature may be the dominant driver of regional hydroclimate variability at these timescales. [77] identified a rapid landscape transformation around 900 CE, recognized by a large $\delta^{13}C$ shift, with no $\delta^{18}O$ change. The change, replicated by Voarintsoa et al., [78] and consistent with regional lake core records [79, 80], was attributed to a switch from C3 to C4 flora and associated with the arrival of slash and burn agriculture for growing grass following the introduction of cattle. Early Holocene speleothems from Anjohibe and Anjokipoty indicate wetter conditions prevailed in the early Holocene, including a wet 8.2 ka event [81]. The apparent absence of speleothem growth between 7.5–2 ka in northern Madagascar suggests dryer conditions during the middle Holocene.

3.3. Southern Africa

3.3.1. The summer rainfall region

Many of the caves in the summer rainfall region are formed in dolomite host rocks which leads to a higher concentration of magnesium in drip waters and common deposition of aragonite speleothems [82]. This affects the isotopic composition, and trace element concentrations including uranium both at initial deposition and where aragonite recrystallizes into secondary calcite [83, 84]. Monitoring of the mineralogy and testing for recrystallization are therefore crucial in these caves to assess the value of a sample for paleoenvironmental studies.

$\delta^{13}C$ values of speleothems from the South African summer rainfall region are traditionally interpreted to reflect shifts of the relative abundance of C3 and C4 plants in the vegetation above the cave, as both types of vegetation are common in the region [85; 7]. Although vegetation changes may also affect $\delta^{13}C$ in northern Namibia/Botswana, multiproxy analyses of the speleothems there (including $\delta^{18}O$, mineralogy, petrography, type of layering, and thickness of lamina) suggest that higher $\delta^{13}C$ values are generally associated with direr conditions and lower values with wetter periods, making PCP a more likely driver [86, 87].

The oldest analyzed speleothems in the southern African summer rainfall region originate from Collapsed Cone at Makapansgat Limeworks and from Buffalo Cave; they indicate the spread of C4 grasses across southern Africa between the end of the Neogene and the early Pleistocene [12,13]. While the initial spread of C4 grasses was probably caused by dropping global levels of atmospheric pCO_2, a subsequent expansion of C4 grasses in the South African summer rainfall region at ~1.7 Ma was caused by drying climates due to the reorganization of tropical circulation [12,13]. Changes in the net water budget, indicated by $\delta^{18}O$ and lamina thickness, follow a precessional periodicity at this time [88, 13].

The last glacial cycle is well represented in speleothem records from this region, starting with a phase of deposition at Wolkberg Cave (58–46 ka) [89], Gladysvale Cave (56–42 ka) [90], and Lobatse Cave (51–43 ka) [91, 92]. Speleothem growth phases and stable isotopic records from Wolkberg Cave and Lobatse Cave support a wet and warm climate with a trend towards drier and cooler conditions from 50 to 45 ka [91, 92, 89]. Speleothem deposition starts at Orumana Cave in northwestern Namibia starts at a similar time (47.5 ka) and lasted at least until 24 ka [86] suggesting more consistently wet conditions here than in northern South Africa. A short second phase of speleothem formation at 40 ka in Wolkberg Cave overlaps with the onset of deposition in Sudwala Cave (40 ka) [93, 89] and renewed speleothem formation at Lobatse Cave (~38 ka) [91, 92]. The period between 35 and 30 ka saw widespread cessation of speleothem deposition in Wonderwerk Cave (33 ka), Echo Cave (30 ka), Sudwala Cave (35 ka), Lobatse Cave (35 ka), and Sterkfontein Caves (after 30 ka) [92, 93, 94, 95, 96]. Evidence of cave flooding at Echo Cave (30 ka) and geochemical proxies and detrital material at Sudwala Cave (35 ka) suggest that wetter conditions are a more likely explanation for the halt of speleothem formation than an aridification of climate [93, 95].

Speleothem deposition resumes at Lobatse Cave at 27 ka with generally cooler conditions than in its first phase of deposition (51–43 ka) and a higher abundance of C4 grasses [91, 92] or drier conditions if $\delta^{13}C$ is interpreted in terms of PCP. Speleothem formation starts at Cold Air Cave and Wonderwerk Cave at ~24 ka with stable isotopes from Wonderwerk indicative of warm and dry conditions [94, 85]. Resumed proxy records at Orumana Cave in Namibia also suggest drier conditions there between 20 and 14.5 ka than during the earlier part of the records (~47–39 ka) [86]. Continued aridification in northern Namibia during the early part of the Antarctic Cold Reversal (ACR) then leads to a hiatus at Orumana Cave at 14.5 ka [86]. A short deposition phase at Drotsky's Cave at 14.5 ka is followed by a hiatus [40]. Cold and dry conditions are also suggested for the ACR (14.7–13.0 ka) in Cold Air Cave and Sudwala Cave [93].

The onset of the Younger Dryas period (~12.9–11.7 ka) is associated with widespread cessation of speleothem deposition (Sudwala: 12.8 ka; Wonderwerk: 13 ka; Cold Air Cave: 12.7 ka) [94, 93, 85]. The Early Holocene is covered by only one speleothem from Cold Air Cave which suggests warm but dry conditions between 10 and 6 ka [85]. During the mid-Holocene, a speleothem from Dante Cave in northeastern Namibia continuously covers the past 4.7 ka [87]. A short-wet period around 3.3 ka ago at Dante Cave is followed by very dry conditions until 1.8 ka, when an abrupt transition to wetter conditions overlaps with the migration of Iron Age herders from northern Africa into southern Africa [87, 97]. Wet conditions are also evident in records from Cold Air Cave between 1.2 and 0.6 ka [85, 99]. The Little Ice Age (~0.7–0.1 ka BP) was cool and dry at Cold Air Cave with the coldest interval centered between 1690 and 1740 CE following the Maunder Minimum [85, 98, 99]. In northern Namibia, however, records from Orumana and Dante Cave suggest very wet conditions especially during the Maunder (305–235 years BP; 1645–1715 CE) and Dalton (160–120 years BP; 1790–1830 CE) minima in solar activity [86, 82].

3.3.2. Year-round rainfall region

The narrow strip along the southern coast of Africa sits at the intersection between the subtropical summer rainfall region and the Mediterranean winter rainfall region and receives rainfall all year round; this region is represented here by four cave sites. A stalagmite from Cango Cave covers the last ~47 ka with a hiatus between ~17 and 6 ka [6]. Both radiocarbon and U-series dates were

measured on the speleothem used in this study and a discrepancy between the dating results was noted [6, 100] for future comparisons of this record to other paleoclimate proxies an update of the age model is recommended. Values of $\delta^{13}C$ at Cango Cave were interpreted to reflect shifts of the proportion of C3 and C4 plants in the vegetation above the cave; $\delta^{18}O$ values only vary by ~1.5‰, with no markable shift between the last glacial and the Holocene [6].

Two studies of speleothem records at Pinnacle Point on the south coast of South Africa, show considerably larger variability of $\delta^{18}O$ than at Cango Cave, albeit during different time intervals. A first record from Crevice Cave covering the interval between 90 and 53 ka [101] was extended by adding speleothem samples from PP29 (112–43 ka) and Staircase Cave (330–130 ka) [39]. The caves at Pinnacle Point are not classical karst caves, but a combination of repetition tests and Hendy tests at the three caves supports environmental factors as being the main drivers of isotopic change [101, 39]. Variations of $\delta^{13}C$ were interpreted as reflecting changes of vegetation above the caves. Monitoring of rainwater $\delta^{18}O$ in the nearby town of Mossel Bay has shown considerable seasonal variations [101, 102]. Changes of the $\delta^{18}O$ values of speleothems therefore have been interpreted in terms of variations in the seasonality of rainfall and associated synoptic conditions [101, 39].

4. Discussion

4.1. Regional speleothem age distributions

Figure 3 shows the distribution of speleothem ages (from the SISAL_v1 records) plotted against time. We discuss here the age distributions of speleothems across the three main regions (North Africa, East Africa and southern Africa, Figure 1) and make some tentative inter-region comparisons.

Speleothem deposition in the North African region appears uneven due to irregular sampling of multiple caves in multiple climatic regions. At caves in the western part of North Africa (Tunisia, Algeria and Morocco) speleothem deposition has mainly been documented during the Holocene, with few ages in the late Pleistocene [46]. Deposition in this region is driven by the temperate westerlies. On glacial-interglacial timescales changes in the volume of ice and the effects of meltwater on oceanic circulation in the north Atlantic can cause major reorganizations of these atmospheric systems which leads to changing relationships between rainfall in northwestern North Africa with other regions around the Mediterranean Sea and in Europe [44, 16, 49].

Preprints (www.preprints.org) | NOT PEER-REVIEWED | Posted: 1 October 2018 doi:10.20944/preprints201810.0016.v1

Peer-reviewed version available at *Quaternary* **2019**, *2*, 4; doi:10.3390/quat2010004

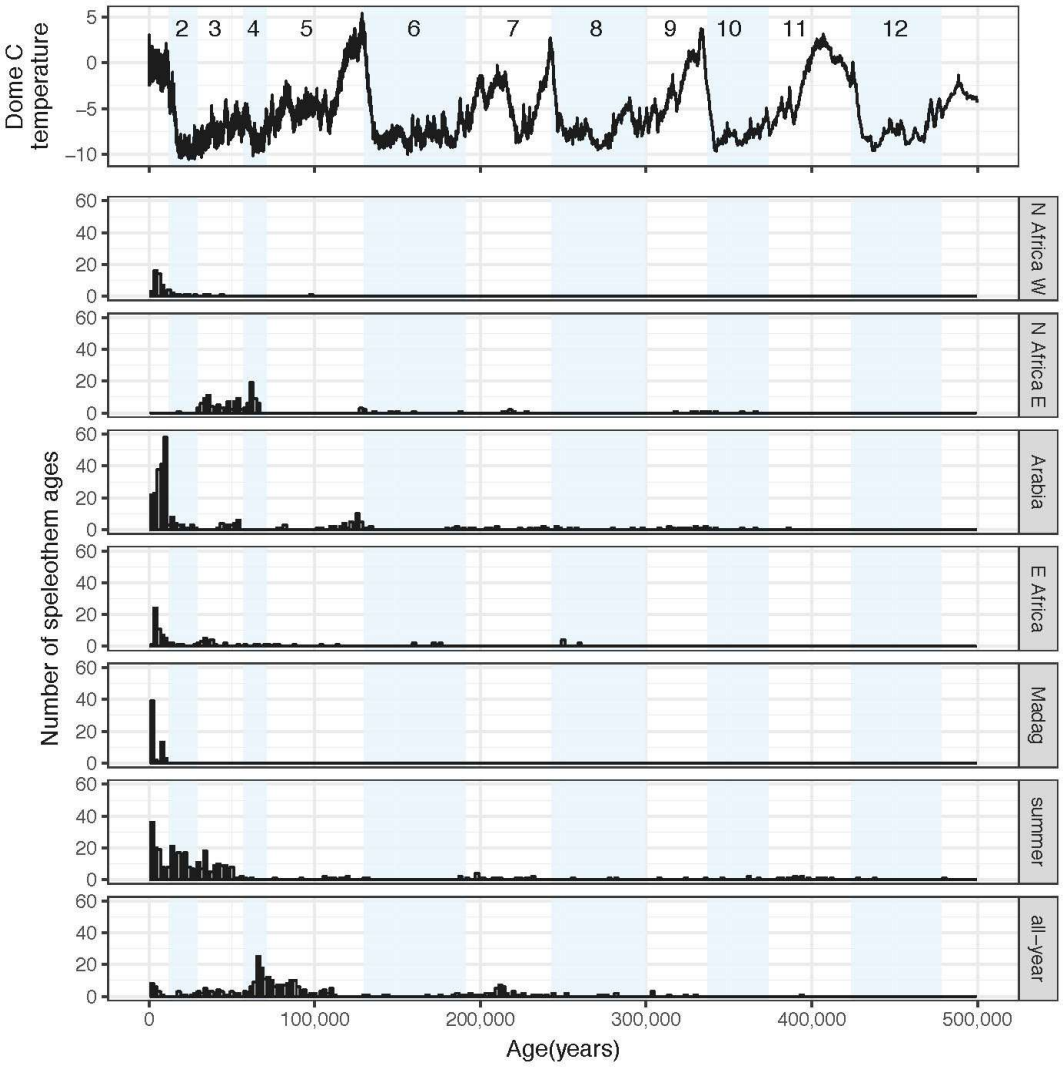

Preprints (www.preprints.org) | NOT PEER-REVIEWED | Posted: 1 October 2018 doi:10.20944/preprints201810.0016.v1

Peer-reviewed version available at Quaternary 2019, 2, 4; doi:10.3390/quat2010004

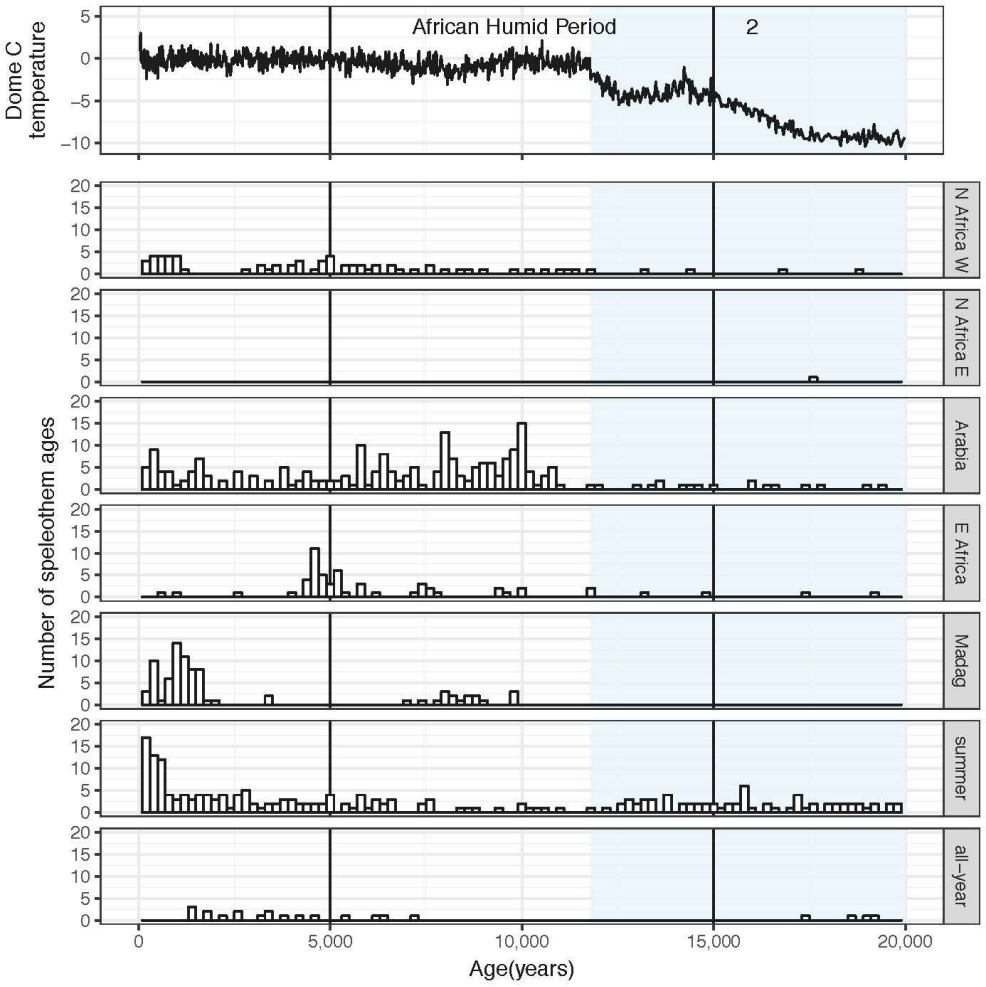

Figure 3. Age distribution histograms of ages measured on speleothems separated by regions indicated in Figure 1: (**a**) for the last 500 ka (left); (**b**) the last 20 ka (right). In both panels: temperature reconstructions (relative to present day) from EPICA Dome C ice core in Antarctica [Jouzel et al., 2007**]**. Light blue shading marks glacial intervals. Numbers at the top of the left panel indicate MIS intervals. Vertical lines in (a) mark the boundaries of the African Humid Period.

In the eastern part of North Africa, speleothem deposition is associated with large scale North African pluvials that lead to the formation of lakes in the now hyperarid interior [17, 15]. These pluvials are usually induced by increased summer insolation on the northern hemisphere and a northward shift of ITCZ rainfall during phases when the boreal summer solstice is close to perihelion (low precession index) [103]. One wet phase identified in Libya has been associated with high obliquity leading to a similar outcome [15]. In extreme cases, the high freshwater runoff from North Africa leads to stratification of the water column in the Eastern Mediterranean Basin and the deposition of sapropel layers [18]. Deposition phases in eastern North Africa with ages of 340 to 317 ka, 219–214 ka, and 130–128 ka overlap with such extreme pluvials (sapropels 10, 8, and 5) [17]. The lack of coverage of younger sapropels might be due to the low number of studies and speleothem samples from the region. The Susah cave record in Libya presents rare evidence of increased effective rainfall in the North African region during parts of the last glacial period. Major deposition periods are out of phase with the monsoonal rainfall registered in Egyptian speleothems and sapropels and minor depositional phases commonly overlap with Greenland warm phases suggesting important influences of Atlantic moisture in this region [15]. Dry periods observed in Gueldaman Cave [16] were also identified in La Mine Cave [44] and other sites surrounding the Mediterranean [104, 105,

106, 107]. These observations indicate that perturbations of the westerlies triggered from high latitudes affected the regional climatic regime across the Mediterranean Basin during the Mid-Holocene.

Speleothem deposition in southern Arabia is mostly centered on interglacial phases and northern hemisphere warm intervals within the Holocene (Figure 3) [55, 52, 56, 57, 63, 54, 108]. The area represents the northernmost extent of the migrations of the ITCZ rainfall belt and the Indian Summer Monsoon [52]. Most of the intervals of deposition in Arabia overlap with deposition in eastern North Africa, but the phases of deposition are longer in Arabia than eastern North Africa. This difference could reflect the more southern position of the Arabian sites where a more frequent or extended influence of the tropical rain belt is likely, or the orographic nature of southern Arabian rainfall. There might also be a difference in the timing of wet periods of the Indian Monsoon System and African pluvial periods. The highest number of speleothems in southern Arabia date to the early Holocene covering the younger half of the African Humid Period between ~10 and 5 ka (Figure 3). This interval is thought to have been humid in large parts of northern Africa and it is associated with sapropel deposition in the Eastern Mediterranean [18]. The lack of speleothems dated to this interval in eastern North Africa, therefore is more likely due to the lack of sufficient sampling rather than a lack of speleothem formation.

The few dates on speleothems in eastern Africa suggest humid conditions in both glacial and interglacial intervals. The limited sampling in Madagascar has, so far, mostly produced samples dating to the last 2ka. The small number of early Holocene samples does not allow for a definitive statement about the depositional phases but is consistent with a northern position of the ITCZ during the African Humid Period (Figure 3).

Speleothem deposition in the southern African summer rainfall region is more common in interglacial phases than in glacials, up until the last glacial phase (Figure 3). Depositional intervals thus generally overlap with those in southern Arabia (Figure 3). The coherence of depositional phases of speleothems from the northern (southern Arabia) and southern (southern African summer rainfall) extremes of the influence of ITCZ migrations supports a generally larger latitudinal range of these migrations during interglacials or a widening of the rainfall belt itself [109, 24]. During glacials, increased polar ice volume and a contraction of tropical circulation systems between equatorward shifted westerlies in both hemispheres may have caused drier climates in these regions. The last glacial phase does however show considerable speleothem formation in the southern African summer rainfall zone (Figure 3) supporting the common assumption that a disproportionate cooling of the larger landmass in the northern hemisphere can cause an overall southward shift of the ITCZ during cold phases [110]. A peak in dating analyses centered at 20 ka during both a southern hemisphere insolation maxima and peak glacial conditions supports both precessional and glacial-interglacial boundary conditions as controls on southern African summer rainfall (Figure 3). The number of speleothems forming in the early Holocene in this region is low compared to the last glacial phase and the mid-late Holocene further supporting dry conditions and a northern position of the ITCZ during much of the African Humid Period (Figure 3).

In the year-round rainfall region of southern Africa, much of the rainfall is associated with connections between tropical and temperate rainfall systems [38]. Speleothem deposition is more common in interglacials, mainly in MIS 5 and 7 (Figure 3a). This may represent the widening of the seasonal latitudinal migration of the ITCZ during interglacials allowing for good connectivity between tropical and temperate low-pressure systems [39]. The largest number of speleothem ages in the year-round rainfall region was, however, measured in early MIS 4 (Figure 3a). A high precession parameter suggests a possible southward shift of the ITCZ. At the same time the westerlies were strengthened [111] which allowed for good connectivity of tropical and temperate rainfall systems [39]. One sample with last glacial to Holocene age was reported from the year-round rainfall region of southern Africa. This sample shows a hiatus in deposition between ~16 and 8 ka [6],

supporting the dry conditions suggested in the southern African speleothem records (Figure 3) and a northward shift of the ITCZ during the African Humid Period.

4.1. Pan African ranges of $\delta^{18}O$ and $\delta^{13}C$

The $\delta^{18}O$ values of African speleothems range mostly from ~0 to ~5‰ except for Dante cave in northwestern Namibia where isotopic values reach lower than -10‰, possibly because of the inland location of the site. In the North African region, the Holocene records from Iflouki, La Mine, and Gueldaman caves show $\delta^{18}O$ signatures close to present Mediterranean vapour $\delta^{18}O$ [112]. The large variability of $\delta^{18}O$ values at Gueldaman cave indicates variable moisture conditions including prominent dry periods during the late-Holocene. The Arabian records (Hoti, Qunf, Defore and Moomi caves) show generally slightly more enriched $\delta^{18}O$ values than the north African records. We also find more isotopic enrichment at Defore Cave compared to Hoti, Moomi and Qunf Caves. This offset confirms that the Arabian and Mediterranean sites are not within the same precipitation system and reflect the short transport distance between Arabian sites and the Indian Ocean. From Arabia southwards to East Africa, $\delta^{18}O$ becomes more depleted (Figure 4a). This spatial pattern may reflect the amount effect commonly observed in monsoonal rainfall [113]. Even during phases when the ITCZ is in a northern position rainfall amounts are lower at the fringes of the monsoon influence (southern Arabia) than in its center (equatorial East Africa), which would lead to the overall higher $\delta^{18}O$ values observed in southern Arabia (Figure 4a). The inverse pattern is however not observed in sites to the south of the equator, with southern African sites (Cold Air cave, Wolkberg cave, Buffalo cave, Lobatse cave and Cango cave) all recording $\delta^{18}O$ values of around -5‰. While this may well be due to sampling bias, it also hints at mechanisms other than the position of the ITCZ and the amount affect driving the $\delta^{18}O$ values.

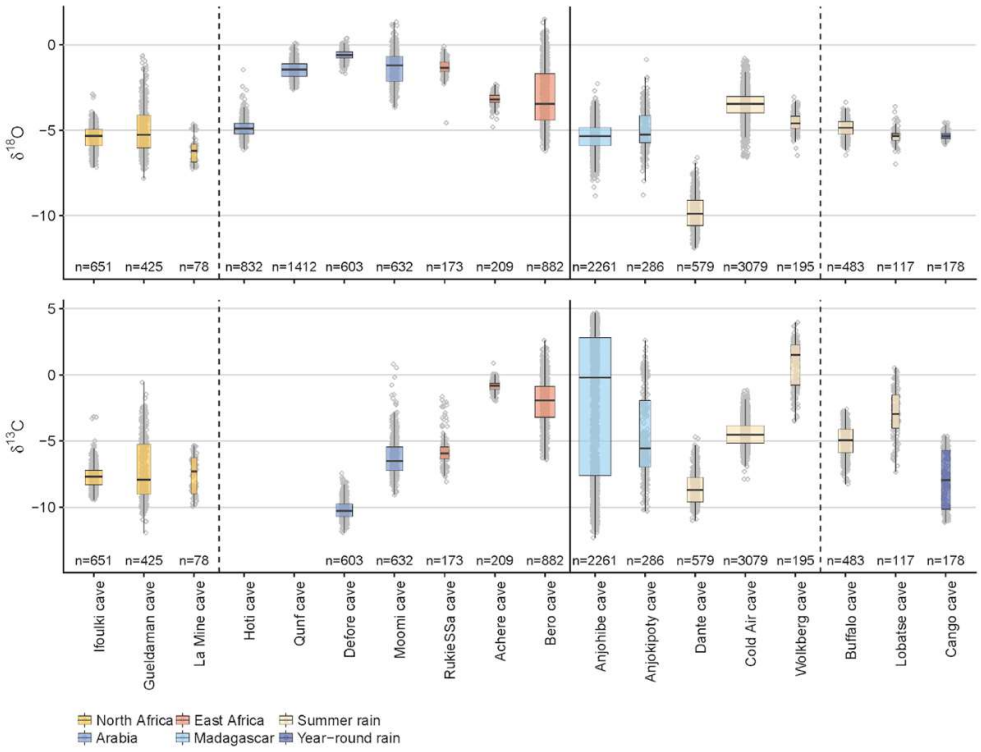

Figure 4. The range of isotope values for each cave in the SISAL_v1 database: (**a**) $\delta^{18}O$; (**b**) $\delta^{13}C$. Sites are arranged by region as indicated in Figure 1 from north to south (left to right). Within the regions, in North Africa, sites are sorted by longitude (west to east), all other regions are sorted internally by latitude. All individual analyses are plotted as grey diamonds, upper and lower hinges of the boxes represent 75 and 25% quantiles, the horizontal line inside the boxes represents the median (50%

quantile). Upper and lower whiskers show the highest and lowest measured values excluding outliers. Analyses with values higher than the 75% quantile plus 1.5 times the interquartile range (distance between first and third quartiles) or lower than the 25% quantile minus 1.5 times the interquartile range are considered outliers. The solid vertical line separates sites on the northern hemisphere (left) from sites on the southern hemisphere (right); sites between the dashed lines are located within the tropics. The width of the boxes is scaled to the number of analyses included in each boxplot. The only records within SISAL_v1 that were excluded from this plot are the normalized stable isotope records from Grotte de Piste.

The $\delta^{13}C$ values of African speleothems range from ~3‰ to -10‰ (Figure 4b). The largest range of values is recorded in northern Madagascar due to human induced land-use change [77]. $\delta^{13}C$ values in North African records range mainly between -10‰ and -5‰ and reflect higher abundance of C4 grasses and/or stronger PCP associated with cool/dry conditions [44, 47, 16]. Speleothem records from southern Arabia and East Africa show a trend towards more positive values closer to the equator (Figure 4b). In southern Africa, $\delta^{13}C$ values at Dante Cave are comparatively low (~-5 to -10 ‰) [87, 82], which also may reflect the inland location of the site. The South African sites (Cold Air Cave, Wolkberg Cave, Buffalo Cave, Lobatse Cave and Cango Cave), to some extent, show a similar trend as the southern Arabian and East African sites with decreasing values with increasing distance from the equator (Figure 4b). This tendency in the data is unexpected, because higher temperature and rainfall in the tropics would be expected to lead to higher soil respiration, and lower $\delta^{13}C$ [44]. This inversion of the expected trend may arise from differences in gas exchange within the cave, which is considered important in Ethiopia [65]. Regardless, this apparently systematic correlation of $\delta^{13}C$ to latitude is an important feature of the data to resolve further.

5. Future research directions

There is great potential for speleothem studies to contribute to open questions concerning African palaeoclimates. As African speleothem records are temporally flashy, continued research should combine these snapshots with other longer term, lower resolution hydroclimate records such as sediment cores from lakes and near shore [114, 115, 116, 117, 75]. We identify three key paleoclimate questions in Africa that stand to benefit from future speleothem research: Firstly, the question of interhemispheric teleconnection vs. see-saw: paleoclimate proxy records from southern and eastern Africa show a complex pattern with some southern hemisphere sites suggesting wet phases during northern hemisphere warm intervals, while others suggest that northern hemisphere cold phases were wet in southern/southeastern Africa [118, 119, 120, 73]. Secondly, the expansion and contraction of desert regions in both hemispheres, the Sahara in the north and Kalahari/Namib in the south; speleothems can be used to investigate changes in the availability of moisture in regions that are now deserts or close to desert areas [51, 54, 121]. Thirdly, Africa is home to the origins of humanity, in both early hominin evolution and the beginnings of cultural modernity. Speleothems from palaeoanthropological and archaeological sites, preserving remains and artifacts of early hominins, as well as modern humans, have been used for dating and the reconstruction of climates [122, 101, 39, 12].

Additional research targets include: a priority to increase the number of African records in the SISAL database for more substantial data analysis, and efforts to re-analyze materials that were sampled in the 80s and 90s, increasing dating accuracies and sampling resolutions of proxies and/or using new proxy methods. We also highlight the large areas of Africa with significant karst regions that remain unexplored, such as West Africa, Angola, Tanzania and central Africa, meaning that there is enormous potential for more speleothem records. West and Central Africa are total greenfield exploration targets, but not necessarily easy, accessible or safe places to work.

6. Conclusions

The number and density of speleothem studies across large parts of Africa is very low because of restrictive bedrock geology and dry climate (Figure 1). Speleothem deposition at the southern and northern extremities of the present day ITCZ migration appears to be more common during late Pleistocene interglacials than during glacial phases suggesting an overall increased latitudinal range of ITCZ migration or a widening of the tropical rainfall belt during interglacials. During glacial phases speleothem deposition is recorded mainly on the hemisphere that has the higher summer insolation as indicated by the precession parameter. Due to the low number of samples and scattered spatial distribution in the African equatorial regions, speleothem records do not yield a reliable picture of how these regions are affected by the changes in the latitudinal range of the ITCZ.

We have focused on U-Th dated speleothem records but, using U-Pb dating, it is possible to go beyond the 500ka cut off of U-Th and explore speleothem records millions of years old. This is particularly pertinent in Africa given the wealth and antiquity of the fossil and archaeological record of human evolution. Using U-Pb dated speleothems from early hominin bearing caves sites, in areas such as the Cradle of Humankind in South Africa, opens up the fascinating possibility of looking at the relationship between human evolution and changes in the past hydroclimate through a local, terrestrial and directly dated archive.

Finally, the speleothems records discussed and analysed here are just the beginning; work is already in progress on the second version of the SISAL database and we intend to include as many new records for the African region as possible. We hope that this contribution serves as both a review of the state of speleothem research in Africa, provides a window into what we do know from this record and a springboard for future research endeavors.

Author Contributions: The first draft of the paper was written by K.B. with input from all other authors. All authors contributed to manuscript editing and revisions.

Funding: This research received no external funding

Acknowledgments: SISAL is a working group of the Past Global Changes (PAGES) programme, and we thank PAGES for their support for this initiative. We would like to especially thank the SISAL members and our speleo-colleagues for contributing their published data to the database and provided additional information when necessary. Specifically, we wish to thank Andy Baker for assisting with the Ethiopia stalagmite section and Jessica Jessica von der Meden for accessing some obscure South African literature.

Conflicts of Interest: The authors declare no conflict of interest.

References

1. Atsawawaranunt, Kamolphat, Harrison, Sandy P., Comas Bru, Laia. SISAL (Speleothem Isotopes Synthesis and Analysis Working Group) database Version 1.0, University of Reading. Dataset **2018a**, DOI: 10.17864/1947.147.
2. Atsawawaranunt, K., Comas-Bru, L., Amirnezhad Mozhdehi, S., Deininger, M., Harrison, S. P., Baker, A., Boyd, M., Kaushal, N., Ahmad, S. M., Ait Brahim, Y., Arienzo, M., Bajo, P., Braun, K., Burstyn, Y., Chawchai, S., Duan, W., Hatvani, I. G., Hu, J., Kern, Z., Labuhn, I., Lachniet, M., Lechleiter, F. A., Lorrey, A., Pérez-Mejías, C., Pickering, R., Scroxton, N., and SISAL Working Group Members. The SISAL database: a global resource to document oxygen and carbon isotope records from speleothems. *Earth System Science Data* **2018b**, DOI: 10.5194/essd-2018-17.
3. Van Hinsbergen, D.J.J., Buiter, S.J.H., Torsvik, T.H., Gaina, C., Webb, S.J. The formation and evolution of Africa from the Archaean to Present: introduction. *Geological Society, London, Special Publications* **2011**, 357(1), 1-8. DOI: 10.1144/SP357.1
4. Chen Z, Auler AS, Bakalowicz M, Drew D, Griger F, Hartmann J, Jiang G, Moosdorf N, Richts A, Stevanovic Z, Veni G, Goldscheider N. The World Karst Aquifer Mapping project: concept, mapping procedure and map of Europe. *Hydrogeology Journal* **2017**, *25(3)*, 771-785.
5. UNEP. *Africa: Atlas of Our Changing Environment*. Division of Early Warning and Assessment (DEWA) United Nations Environment Programme (UNEP), New York, USA, 2008. ISBN: 978-92-807-2871-2.
6. Talma, A.S., Vogel, J.C. Late Quaternary Paleotemperatures derived from a Speleothem from Cango Caves, Cape Province, South Africa. *Quaternary Research* **1992**, *37*, 203–213. DOI: 10.1016/0033-5894(92)90082-T
7. Talma, A.S., Vogel, J.C., Partridge, T.C. Isotopic contents of some Transvaal speleothems and their palaeoclimatic significance. South African Journal of Science **1974**, *70*, 135–140.
8. Woodhead, J., Hellstrom, J., Maas, R., Drysdale, R., Zanchetta, G., Devine, P., Taylor, E. U-Pb geochronology of speleothems by MC-ICPMS, *Quaternary Geochronology* **2006**, *1*, 208-221. DOI: 10.1016/j.quageo.20 09.12.0 02.
9. Walker, J., Cliff, R.A., Latham, A.G. U-Pb isotopic age of the StW 573 hominid from Sterkfontein, South Africa, *Science* **2006**, *314*, 1592-1594. DOI: 10.1126/science.1132916.
10. Pickering, R., Kramers, J.D., Partridge, T., Kodolanyi, J., Pettke, T. U–Pb dating of calcite–aragonite layers in speleothems from hominin sites in South Africa by MC-ICP-MS, *Quaternary Geochronology* **2010**, *5*, 544-558. DOI: 10.1016/j.quageo.2009.12.004.
11. Pickering, R., Herries, A.I.R., Woodhead, J.D., Hellstrom, J.C., Green, H.E., Paul, P., Ritzman, T., Strait, D.S., Schoville, B.J., Hancox, P.J. U-Pb dated flowstones restrict South African early hominin record to dry climate phases. **2018**, In Press.
12. Hopley, P.J., Weedon, G.P., Marshall, J.D., Herries, A.I.R., Latham, A.G., Kuykendall, K.L. High- and low-latitude orbital forcing of early hominin habitats in South Africa. *Earth and Planetary Science Letters* **2007a**, *256*, 419–432. DOI: 10.1016/j.epsl.2007.01.031.
13. Hopley, P.J., Marshall, J.D., Weedon, G.P., Latham, A.G., Herries, A.I.R., Kuykendall, K.L. Orbital forcing and the spread of C4 grasses in the late Neogene: stable isotope evidence from South African speleothems. *Journal of Human Evolution* **2007b**, *53*, 620–634. DOI: 10.1016/J.JHEVOL.2007.03.007.
14. Knippertz, P., Christoph, M., Speth, P. Long-term precipitation variability in Morocco and the link to the large-scale circulation in recent and future climates. *Meteorology and Atmospheric Physics* **2003**, *83*, 67–88. DOI: 10.1007/s00703-002-0561-y.
15. Hoffmann, D.L., Rogerson, M., Spötl, C., Luetscher, M., Vance, D., Osborne, A.H., Fello, N.M. and Moseley, G.E. Timing and causes of North African wet phases during MIS 3 and implications for Modern Human migration. *Nature Scientific Reports* **2016**, *6*, 36367. DOI: 10.1038/srep36367.
16. Ruan, J., Kherbouche, F., Genty, D., Blamart, D., Cheng, H., Dewilde, F., Hachi, S., Edwards, R., Régnier, E. and Michelot, J.-L. Evidence of a prolonged drought ca. 4200 yr BP correlated with prehistoric settlement abandonment from the Gueldaman GLD1 cave, Northern Algeria. *Climate of the Past* **2016**, *12*, 1-14. DOI: 10.5194/cp-12-1-2016.
17. El-Shenawy, M.I., Kim, S.-T., Schwarcz, H.P., Asmerom, Y. and Polyak, V.J. Speleothem evidence for the greening of the Sahara and its implications for the early human dispersal out of sub-Saharan Africa. *Quaternary Science Reviews* **2018**, *188*, 67-76. DOI: 10.1016/j.quascirev.2018.03.016.

18. Rohling, E.J., Marino, G., Grant, K.M. Mediterranean climate and oceanography, and the periodic development of anoxic events (sapropels). *Earth-Science Reviews* **2015**, *143*, 62–97. DOI: 10.1016/J.EARSCIREV.2015.01.008.
19. deMenocal, P. Ortiz, J., Guilderson, T., Adkins, J., Sarnthein, M., Baker, L, Yarusinsky, M. Abrupt onset and termination of the African Humid Period: rapid climate responses to gradual insolation forcing. Quaternary Science Reviews 2000, 19, 347-361. DOI: 10.1016/S0277-3791(99)00081-5.
20. Armitage S.J., Drake N.A., Stokes S., El-Hawat A., Salem M.J., White K., Turner P., McLaren S.J. Multiple phases of North African humidity recorded in lacustrine sediments from the Fazzan Basin, Libyan Sahara. Quaternary Geochronology 2007, 2,181-186. DOI: 10.1016/j.quageo.2006.05.019.
21. Nicoll, K. Recent environmental change and prehistoric human activity in Egypt and Northern Sudan. *Quaternary Science Reviews* **2004**, *23*(5-6), 561-580. DOI: 10.1016/j.quascirev.2003.10.004
22. Hoelzmann, P., Jolly, D., Harrison, S. P., Laarif, F., Bonnefille, R., Pachur, H. J. Mid-Holocene land-surface conditions in northern Africa and the Arabian Peninsula: A data set for the analysis of biogeophysical feedbacks in the climate system. *Global biogeochemical cycles* **1998**, *12*, 35-51. DOI: 10.1029/97GB02733
23. Swezey, C. Eolian sediment responses to late Quaternary climate changes: temporal and spatial patterns in the Sahara. *Palaeogeography, Palaeoclimatology, Palaeoecology* **2001**, 167.1-2, 119-155. DOI: 10.1016/S0031-0182(00)00235-2.
24. Singarayer, J. S., Burrough, S. L. Interhemispheric dynamics of the African rainbelt during the late Quaternary. Quaternary Science Reviews, **2015**, *124*, 48 - 67. DOI: 10.1016/j.quascirev.2015.06.021.
25. Nicholson, S.E. A review of climate dynamics and climate variability in Eastern Africa. In: The Limnology, Climatology and Paleoclimatology of the East African Lakes; ed., Johnson, T.C., Odada, E.O., Gordon and Breach, Amsterdam, **1996**, pp. 25-56.
26. Black, E., Slingo, J., Sperber, K.R. An Observational Study of the Relationship between Excessively Strong Short Rains in Coastal East Africa and Indian Ocean SST. *Monthly Weather Review* **2003,** *131*, 74–94. DOI: 10.1175/1520-0493(2003)131<0074:AOSOTR>2.0.CO;2
27. Goddard, L., Graham, N.E. Importance of the Indian Ocean for simulating rainfall anomalies over eastern and southern Africa. *Journal of Geophysical research* **1999**, *104*, 19099–19116. DOI:10.1029/1999JD900326.
28. Ummenhofer, C.C., Gupta, Sen, A., England, M.H., Reason, C.J.C. Contributions of Indian Ocean Sea Surface Temperatures to Enhanced East African Rainfall. *American Meteorological Society* **2009**, *22*, 993–1013. DOI:10.1175/2008JCLI2493.1
29. Ummenhofer, C.C., Kulüke, M., Tierney, J.E. Extremes in East African hydroclimate and links to Indo-Pacific variability on interannual to decadal timescales. *Climate Dynamics* **2017**, 1–21. DOI:10.1007/s00382-017-3786-71.
30. Saji, N.H., Goswami, B.N., Vinayachandran, P.N., Yamagata, T., 1999. A dipole mode in the tropical Indian Ocean. *Nature* **1999**, *401*, 360.
31. Webster, P.J., Moore A.M., Loschnigg J.P., Leben R.R. Coupled ocean–atmosphere dynamics in the Indian Ocean during 1997–98. *Nature* **1999**, 401, 356-360. DOI:/10.1038/43848;
32. Zinke, J., Pfeiffer, M., Timm, O., Dullo, W.C., & Brummer, G.J.A. Western Indian Ocean marine and terrestrial records of climate variability: a review and new concepts on land–ocean interactions since AD 1660. *International Journal of Earth Sciences* **2009**, *98*, 115. DOI:10.1007/s00531-008-0365-5;
33. Konecky, B., Russell, J.M., Vuille, M., Rehfeld, K. The Indian Ocean Zonal Mode over the past millennium in observed and modeled precipitation isotopes. *Quaternary Science Reviews* **2014**, *103*, 1–18. DOI: 10.1016/j.quascirev.2014.08.019;
34. Weldeab, S., Lea, D.W., Oberhänsli, H., Schneider, R.R. Links between southwestern tropical Indian Ocean SST and precipitation over southeastern Africa over the last 17 kyr. *Palaeogeography Palaeoclimatology Palaeoecology* **2014**, *410*, 200–212. DOI: 10.1016/j.palaeo.2014.06.001.
35. Hansingo, K., Reason, C.J.C. Modelling the atmospheric response to SST dipole patterns in the South Indian Ocean with a regional climate model. *Meteorology and Atmospheric Physics* **2008**, *100*, 37–52. DOI: 10.1007/s00703-008-0294-7
36. Van Heerden, J., Taljaard, J.J. Africa and Surrounding Waters. *Meteorology of the Southern Hemisphere*, American Meteorological Society, Boston, MA 1998, 141–174.
37. Collins, J.A., Schefuß, E., Heslop, D., Mulitza, S., Prange, M., Tjallingii, R., Dokken, T.M., Huang, E., Mackensen, A., Schulz, M., Tian, J., Zarriess, M., Wefer, G. Interhemispheric symmertry of the tropical African rainbelt over the past 23,000 years. *Nature Geoscience* **2011**, *4*, 42–45. DOI: 10.1038/ngeo1039

38. Engelbrecht CJ, Landman WA, Engelbrecht FA, Malherbe J. A synoptic decomposition of rainfall over the Cape south coast of South Africa. *Climate Dynamics* **2015**, *44(9)*, 2589–2607.
39. Braun, K., Bar-Matthews, M., Matthews, A., Ayalon, A., Cowling, R.M., Karkanas, P., Fisher, E.C., Dyez, K.A., Zilberman, T., Marean, C.W. Late Pleistocene records of speleothem stable isotopic compositions from Pinnacle Point on the South African south coast show close climate connection with rainfall in the interior. *Quaternary Research* **2018**, in press. DOI: 10.1017/qua.2018.61.
40. Brook, G.A., Burney, D.A., Cowart, J.B. Desert paleoenvironmental data from cave speleothems with examples from the Chihuahuan, Solmali-Chalbi, and Kalahari deserts. *Palaeogeography, Palaeoclimatology, Palaeoecology* **1990**, *76*, 311–329. DOI: 10.1016/0031-0182(90)90118-Q.
41. Fairchild, I.J., and Baker A. *Speleothem science: from process to past environments*. Ed. John Wiley & Sons, Chichester, UK, 2012; 432 p., ISBN: 978-1-4051-9620-8.
42. de Lamotte, D.F., Leturmy, P., Missenard, Y., Khomsi, S., Ruiz, G., Saddiqi, O., Guillocheau, F. and Michard, A. Mesozoic and Cenozoic vertical movements in the Atlas system (Algeria, Morocco, Tunisia): An overview. *Tectonophysics* **2009**, *475*, 9-28. DOI: 10.1016/j.tecto.2008.10.024.
43. Rifai, R.I. Reconstruction of the Middle Pleistocene climate of south Mediterranean using the Wadi Sannur speleothem, eastern Desert, Egypt. *Carbonates and evaporites* **2007**, *22*, 73. DOI: 10.1007/BF03175847
44. Genty, D., Blamart, D., Ghaleb, B., Plagnes, V., Causse, C., Bakalowicz, M., Zouari, K., Chkir, N., Hellstrom, J., Wainer, K. and Bourges, F. Timing and dynamics of the last deglaciation from European and North African $\delta^{13}C$ stalagmite profiles-comparison with Chinese and South Hemisphere stalagmites. *Quaternary Science Reviews* **2006**, *25*, 2118-2142. DOI: 10.1016/j.quascirev.2006.01.030.
45. Rohling, E.J. and De Rijk, S. Holocene Climate Optimum and Last Glacial Maximum in the Mediterranean: the marine oxygen isotope record. *Marine Geology* **1999**, *153*, 57-75. DOI: 10.1016/S0025-3227(98)00020-6.
46. Wassenburg, J.A., Immenhauser, A., Richter, D.K., Jochum, K.P., Fietzke, J., Deininger, M., Goos, M., Scholz, D. and Sabaoui, A. Climate and cave control on Pleistocene/Holocene calcite-to-aragonite transitions in speleothems from Morocco: elemental and isotopic evidence. *Geochimica et Cosmochimica Acta* **2012**, *92*, 23-47. DOI: 10.1016/j.gca.2012.06.002.
47. Ait Brahim, Y., Cheng, H., Sifeddine, A., Wassenburg, J.A., Cruz, F.W., Khodri, M., Sha, L., Pérez-Zanón, N., Beraaouz, E.H., Apaéstegui, J., Guyot, J.-L., Jochum, K.P. and Bouchaou, L. Speleothem records decadal to multidecadal hydroclimate variations in southwestern Morocco during the last millennium. *Earth and Planetary Science Letters* **2017**, *476*, 1-10, DOI: 10.1016/j.epsl.2017.07.045.
48. Wassenburg, J., Immenhauser, A., Richter, D., Niedermayr, A., Riechelmann, S., Fietzke, J., Scholz, D., Jochum, K., Fohlmeister, J. and Schröder-Ritzrau, A. Moroccan speleothem and tree ring records suggest a variable positive state of the North Atlantic Oscillation during the Medieval Warm Period. *Earth and Planetary Science Letters* **2013**, *375*, 291-302. DOI: 10.1016/j.epsl.2013.05.048.
49. Wassenburg, J.A., Dietrich, S., Fietzke, J., Fohlmeister, J., Jochum, K.P., Scholz, D., Richter, D.K., Sabaoui, A., Spötl, C., Lohmann, G., Andreae, Meinrat O. and Immenhauser, A. Reorganization of the North Atlantic Oscillation during early Holocene deglaciation. *Nature Geoscience* **2016**, *9*, 602. DOI: 10.1038/ngeo2767.
50. Burns, S.J., Matter, A., Frank, N., Mangini, A. Speleothem-based paleoclimate record from northern Oman. *Geology* **1998**, *26*, 499. DOI:10.1130/0091-7613(1998)026<0499:SBPRFN>2.3.CO;2.
51. Burns, S.J., Fleitmann, D., Matter, A., Neff, U., Mangini, A. Speleothem evidence from Oman for continental pluvial events during interglacial periods. *Geology* **2001**, *29*, 623–626. DOI: 10.1130/0091-7613(2001)029<0623:SEFOFC>2.0.CO;2
52. Fleitmann, D., Burns, S.J., Neff, U., Mangini, A., Matter, A. Changing moisture sources over the last 330,000 years in Northern Oman from fluid-inclusion evidence in speleothems. *Quaternary Research* **2003a**, *60*, 223–232. doi:10.1016/S0033-5894(03)00086-3.
53. Neff, U., Burns, S.J., Mangini, A., Mudelsee, M., Fleitmann, D., Matter, A. Strong coherence between solar variability and the monsoon in Oman between 9 and 6 kyr ago. *Nature* **2001**, *411*, 290–293. DOI: 10.1038/35077048.
54. Fleitmann, D., Burns, S.J., Pekala, M., Mangini, A., Al-Subbary, A., Al-Aowah, M., Kramers, J., Matter, A. Holocene and Pleistocene pluvial periods in Yemen, southern Arabia. *Quaternary Science Reviews* **2011**, *30*, 783–787. DOI: 10.1016/j.quascirev.2011.01.004.
55. Burns, S.J., Fleitmann, D., Mudelsee, M., Neff, U., Matter, A., Mangini, A. A 780-year annually resolved record of Indian Ocean monsoon precipitation from a speleothem from south Oman. J*ournal of Geophysical research* **2002**, *107*. DOI: 10.1029/2001JD001281;

56. Fleitmann, D., Burns, S.J., Mudelsee, M., Neff, U., Kramers, J., Mangini, A., Matter, A. Holocene Forcing of the Indian Monsoon Recorded in a Stalagmite from Southern Oman. *Science* **2003b,** *300*, 1737–1739. DOI:10.1126/science.1083130.
57. Fleitmann, D., Burns, S.J., Neff, U., Mudelsee, M., Mangini, A., Matter, A. Palaeoclimatic interpretation of high-resolution oxygen isotope profiles derived from annually laminated speleothems from Southern Oman. *Quaternary Science Reviews* **2004**, *23*, 935–945. DOI: 10.1016/j.quascirev.2003.06.019.
58. Burns, S.J., Fleitmann, D., Matter, A., Kramers, J., Al-Subbary, A.A. Indian Ocean Climate and an Absolute Chronology over Dansgaard/Oeschger Events 9 to 13. *Science* **2003**, *301*, 1365–1367. DOI: 10.1126/science.1086227.
59. Shakun, J.D., Burns, S.J., Fleitmann, D., Kramers, J., Matter, A., Al-Subary, A. A high-resolution, absolute-dated deglacial speleothem record of Indian Ocean climate from Socotra Island, Yemen. *Earth and Planetary Science Letters* **2007**, *259*, 442–456. DOI: 10.1016/j.epsl.2007.05.004.
60. Dansgaard, W., Johnsen, S.J., Clausen, H.B., Dahl-Jensen, D., Gundestrup, N.S., Hammer, C.U., Hvidberg, C.S. Evidence for general instability of past climate from a 250-kyr ice-core record. *Nature* **1993**, 364, 218–220. DOI: 10.1038/364218a0.
61. North Greenland Ice Core Project members. High-resolution climate record of Northern Hemisphere climate extending into the Last Interglacial period. *Nature* **2004**, 431, 147–151. DOI: 10.1038/nature02805
62. Van Rampelbergh, M., Fleitmann, D., Verheyden, S., Cheng, H., Edwards, L., De Geest, P., DeVleeschouwer, D., Burns, S.J., Matter, A., Claeys, P., Keppens, E. Mid- to late Holocene Indian Ocean Monsoon variability recorded in four speleothems from Socotra Island, Yemen. *Quaternary Science Reviews* **2013**, *65*, 129–142. DOI: 10.1016/j.quascirev.2013.01.016.
63. Fleitmann, D., Burns, S.J., Mangini, A., Mudelsee, M., Kramers, J., Villa, I., Neff, U., Al-Subbary, A.A., Buettner, A., Hippler, D., Matter, A. Holocene ITCZ and Indian monsoon dynamics recorded in stalagmites from Oman and Yemen (Socotra). *Quaternary Science Reviews* **2007**, *26*, 170–188. DOI: 10.1016/j.quascirev.2006.04.012.
64. Asrat, A., Baker, A., Mohammed, M.U., Leng, M.J., Calsteren, P.V., Smith, C. A high-resolution multi-proxy stalagmite record from Mechara, Southeastern Ethiopia: palaeohydrological implications for speleothem palaeoclimate reconstruction. *Journal of Quaternary Science* **2007**, *22*, 53–63, DOI: 10.1002/jqs.1013.
65. Baker, A., Asrat, A., Fairchild, I.J., Leng, M.J., Thomas, L., Widmann, M., Jex, C.N., Buwen Dong, van Calsteren, P., Bryant, C. Decadal-scale rainfall variability in Ethiopia recorded in an annually laminated, Holocene-age, stalagmite. *The Holocene* **2010**, *20*, 827–836. DOI:10.1177/0959683610365934
66. Asrat, A., Baker, A., Leng, M.J., Hellstrom, J., Mariethozm G., Boomer, I., Yu, D., Jex, C.N., Gunn, J. High-resolution stalagmite evidence of paleoclimatic change in Ethiopia around the last interglacial. *Quaternary Science Reviews* **2018**, in press.
67. Baker, A., Asrat, A., Fairchild, I.J., Leng, M.J., Wynn, P.M., Bryant, C., Genty, D., Umer, M. Analysis of the climate signal contained within $\delta^{18}O$ and growth rate parameters in two Ethiopian stalagmites. *Geochimica et Cosmochimica Acta* **2007**, *71*, 2975–2988. DOI: 10.1016/j.gca.2007.03.029
68. Asrat, A., Baker, A., Leng, M.J., Gunn, J., Umer, M. Environmental monitoring in the Mechara caves, Southeastern Ethiopia: implications for speleothem palaeoclimate studies. I*nternational Journal of Speleology* **2008**, *37*, 207-220, DOI:10.5038/1827-806X.37.3.5.
69. Blyth, A.J., Asrat, A., Baker, A., Gulliver, P., Leng, M.J., Genty, D. A new approach to detecting vegetation and land-use change using high-resolution lipid biomarker records in stalagmites. *Quaternary Research* **2007**, *68*, 314–324. DOI: 10.1016/j.yqres.2007.08.002
70. Holmgren, K., Karlén, W., Lauritzen, S.E., Lee Thorp, J.A., Partridge, T.C., Shaw, P.A., Tyson, P.D. Speleochronology, stable isotopes and laminae analysis of stalagmites from southern Africa, in: *Proceedings of the International Congress on Speleology*, La Chaux-de-Fond, Switzerland, 10-17-8-1997; Pierre-Yves Jeanin ed., Speleo Projects, La Chaux-de-Fonds, Switzerland, 1997, pp. 55–56.
71. Lundblad, K., Holmgren, K. Palaeoclimatological survey of stalagmites from coastal areas in Tanzania. *Geografiska Annaler* 2005, Series A.
72. Brook, G.A., Rafter, M.A., Railsback, L.B., Sheen, S.-W., Lundberg, J. A high-resolution proxy record of rainfall and ENSO since AD 1550 from layering in stalagmites from Anjohibe Cave, Madagascar. *The Holocene* **1999**, *9*, 695–705. DOI:10.1191/095968399677907790
73. Scroxton, N., Burns, S.J., McGee, D., Hardt, B., Godfrey, L.R., Ranivoharimanana, L., Faina, P. Hemispherically in-phase precipitation variability over the last 1700 years in a Madagascar speleothem record. *Quaternary Science Reviews* **2017**, *164*, 25–36. DOI: 10.1016/j.quascirev.2017.03.017.

74. Verschuren, D., Laird, K. R., & Cumming, B. F. Rainfall and drought in equatorial east Africa during the past 1,100 years(2000). Rainfall and drought in equatorial east Africa during the past 1,100 years. *Nature* **2000**, *403*(6768), 410.
75. Tierney, J.E., Smerdon, J.E., Anchukaitis, K.J., Seager, R. Multidecadal variability in East African hydroclimate controlled by the Indian Ocean. *Nature* **2013**, *493*, 389–392. DOI:10.1038/nature117851.
76. Buckles, Laura K., Dirk Verschuren, Johan WH Weijers, Christine Cocquyt, Maarten Blaauw, and Jaap S. Sinninghe Damsté. Interannual and (multi-) decadal variability in the sedimentary BIT index of Lake Challa, East Africa, over the past 2200 years: assessment of the precipitation proxy. *Climate of the Past* **2016**, 12, 5, 1243-1262.
77. Burns, S.J., Godfrey, L.R., Faina, P., McGee, D., Hardt, B., Ranivoharimanana, L., Randrianasy, J. Rapid human-induced landscape transformation in Madagascar at the end of the first millennium of the Common Era. *Quaternary Science Reviews* **2016**, *134*, 92–99. DOI: 10.1016/j.quascirev.2016.01.007
78. Voarintsoa, N.R.G., Wang, L., Railsback, L.B., Brook, G.A., Liang, F., Cheng, H., Edwards, R.L. Multiple proxy analyses of a U/Th-dated stalagmite to reconstruct paleoenvironmental changes in northwestern Madagascar between 370 CE and 1300 CE. *Palaeogeography, Palaeoclimatology, Palaeoecology* **2017a**, *469*, 138–155. DOI: 10.1016/j.palaeo.2017.01.003.
79. Burney, D.A. Late Holocene Vegetational Change in Central Madagascar. *Quaternary Research* **1987**, *28*, 130–143. DOI: 10.1016/0033-5894(87)90038-X.
80. Matsumoto, K., Burney, D.A. Late Holocene environments at Lake Mitsinjo, northwestern Madagascar:. *The Holocene* **1994**, *4(1)*, 16-24. DOI: 10.1177/095968369400400103.
81. Voarintsoa, N.R.G., Railsback, L.B., Brook, G.A., Wang, L., Kathayat, G., Cheng, H., Li, X., Edwards, R.L., Rakotondrazafy, A.F.M., Madison Razanatseheno, M.O. Three distinct Holocene intervals of stalagmite deposition and nondeposition revealed in NW Madagascar, and their paleoclimate implications. *Climate of the Past* **2017b**, *13*, 1771–1790. DOI: 10.5194/cp-13-1771-2017.
82. Carbol, P. and Coudray, J. Climatic fluctuations influence the genesis and diagenesis of carbonate speleothems in southwest France. *National Speleological Society Bulletin* **1982**, *44*, 112-117.
83. Hopley, P.J., Marshall, J.D., Latham, A.G. Speleothem preservation and diagenesis in South African hominin sites: implications for paleoenvironments and geochronology. *Geoarchaeology* **2009**, *24*, 519–547. DOI: 10.1002/gea.20282.
84. Ortega, R., Maire, R., Devès, G., Quinif, Y. High-resolution mapping of uranium and other trace elements in recrystallized aragonite–calcite speleothems from caves in the Pyrenees (France): Implication for U-series dating. *Earth and Planetary Science Letters* **2005**, *237(3–4)*, 911–923. DOI: 10.1016/j.epsl.2005.06.045.
85. Holmgren, K., Lee-Thorp, J.A., Cooper, G.R.J., Lundblad, K., Partridge, T.C., Scott, L., Sithaldeen, R., Talma, A.S., Tyson, P.D. Persistent millennial-scale climatic variability over the past 25,000 years in Southern Africa. *Quaternary Science Reviews* **2003**, *22*, 2311–2326. DOI: 10.1016/s0277-3791(03)00204.
86. Railsback, L.B., Brook, G.A., Liang, F., Marais, E., Cheng, H., Edwards, R. A multi-proxy stalagmite record from northwestern Namibia of regional drying with increasing global-scale warmth over the last 47 kyr: The interplay of a globally shifting ITCZ with regional currents, winds, and rainfall. *Palaeogeography, Palaeoclimatology, Palaeoecology* **2016**, *461*, 109–121. DOI: 10.1016/j.palaeo.2016.08.014.
87. Slettern, H.R., Railsback, L.B., Liang, F., Brook, G.A., Marais, E., Hardt, B.F., Cheng, H., Edwards, R.L. A petrographic and geochemical record of climate change over the last 4600 years from a northern Namibia stalagmite, with evidence of abruptly wetter climate at the beginning of southern Africa's Iron Age. *Palaeogeography, Palaeoclimatology, Palaeoecology* **2013**, *376*, 149–162. DOI: 10.1016/j.palaeo.2013.02.030.
88. Hopley, P.J., Weedon, G.P., Brierley, C.M., Thrasivoulou, C., Herries, A.I.R., Dinckal, A., Richards, D.A., Nita, D.C., Parrish, R.R., Roberts, N.M.W., Sahy, D., Smith, C.L. Orbital precession modulates interannual rainfall variability, as recorded in an Early Pleistocene speleothem. *Geology* **2018**, DOI: 10.1130/G45019.1
89. Holzkämper, S., Holmgren, K., Lee-Thorp, J.A., Talma, A.S., Mangini, A., Partridge, T.C.,. Late Pleistocene stalagmite growth in Wolkberg Cave, South Africa. *Earth Planetary Science Letters* **2009**, *282*, 212–221. DOI:10.1016/j.epsl.2009.03.016
90. Pickering, R., Hancox, P.J., Lee-Thorp, J.A., Grün, R., Graham, E.M., McCulloch, M.T., Berger, L.R. Stratigraphy, U-Th chronology, and paleoenvironments at Gladysvale Cave: insights into the climatic control of South African hominin-bearing cave deposits. *Journal of Human Evolution* **2007**, *53*, 602–619.1.
91. Holmgren, K., Karlén, W., Shaw, P.A. Paleoclimatic Significance of the Stable Isotopic Composition and Petrology of a Late Pleistocene Stalagmite from Botswana. *Quaternary Research* **1995**, *43*, 320–328. DOI:10.1006/qres.1995.1038.

92. Holmgren, K., Lauritzen, S.-E., Possnert, G. $^{230}Th/^{234}U$ and ^{14}C dating of a late Pleistocene stalagmite in Lobatse II Cave, Botswana. *Quaternary Science Reviews* **1994,** *13*, 111–119. DOI:10.1016/0277-3791(94)90036-1.
93. Green, H., Pickering, R., Drysdale, R.N., Johnson, B.C., Hellstrom, J.C., Wallace, M. Evidence for global teleconnections in a late Pleistocene speleothem record of water balance and vegetation change at Sudwala Cave, South Africa. *Quaternary Science Reviews* **2015**, *110*, 114–130. DOI: 10.1016/j.quascirev.2014.11.016.
94. Brook, G.A., Scott, L., Railsback, L.B., Goddard, E.A. A 35 ka pollen and isotope record of environmental change along the southern margin of the Kalahari from a stalagmite and animal dung deposits in Wonderwerk Cave, South Africa. *Journal of Arid Environments* **2010**, *74*, 870–884. DOI: 10.1016/j.jaridenv.2009.11.006
95. Brook, G.A. Stratigraphic evidence of quaternary climatic change at Echo Cave, Transvaal, and a paleoclimatic record for Botswana and northeastern South Africa. *CATENA* **1982**, *9*, 343–351. DOI:10.1016/0341-8162(82)90008-X
96. Brook, G.A., Cowart, J.B., Brandt, S.A., Scott, L. Quaternary climatic change in southern and eastern Africa during the last 300 ka: The evidence from caves in Somalia and the Transvaal region of South Africa. *Zeitschrift für Geomorphologie* **1997**, *108*, 15–48.
97. Vogel, J.C., Fuls, A. Spatial Distribution of Radiocarbon Dates for the Iron Age in Southern Africa. *South African Archaeological Bulletin* **1999**, *54*, 97. DOI:10.2307/3889287
98. Lee-Thorp, J.A., Holmgren, K., Lauritzen, S.-E., Linge, H., Moberg, A., Partridge, T.C., Stevenson, C., Tyson, P.D. Rapid climate shifts in the southern African interior throughout the Mid to Late Holocene. *Geophysical Research Letters* **2001**, *28*, 4507–4510. DOI:10.1029/2000gl012728.
99. Sundqvist, H.S., Holmgren, K., Fohlmeister, J., Zhang, Q., Bar-Matthews, M., Spötl, C., Kornich, H. Evidence of a large cooling between 1690 and 1740 AD in southern Africa. *Nature Scientific Reports* **2013**, *3*, 1767. DOI: 10.1038/srep01767
100. Vogel, J.C. ^{14}C Variations During the Upper Pleistocene. *Radiocarbon* **1983**, *25*, 213–218. DOI: 10.1017/S0033822200005506.
101. Bar-Matthews, M., Marean, C.W., Jacobs, Z., Karkanas, P., Fisher, E.C., Herries, A.I.R., Brown, K.S., Williams, H.M., Bernatchez, J.A., Ayalon, A., Nilssen, P.J. A high resolution and continuous isotopic speleothem record of paleoclimate and paleoenvironment from 90-53 ka from Pinnacle Point on the south coast of South Africa. *Quaternary Science Reviews* **2010**, *29*, 2131-2145. DOI: 10.1016/j.quascirev.2010.05.009
102. Braun, K., Bar-Matthews, M., Ayalon, A., Zilberman, T., Matthews, A. Rainfall isotopic variability at the intersection between winter and summer rainfall regimes in coastal South Africa (Mossel Bay, Western Cape Province). *South African Journal of Geology* **2017**, *120*, 323–340. DOI:10.25131/gssajg.120.3.323
103. Laskar J., Robutel, P., Joutel, F., Gastineau, M., Correia, A. C. M., Levrard, B. A long-term numerical solution for the insolation quantities of the Earth. *Astronomy & Astrophysics* **2004**, *428*, 261–285. DOI: 10.1051/0004-6361:20041335.
104. Zanchetta, G., Bar-Matthews, M., Drysdale, R. N., Lionello, P., Ayalon, A., Hellstrom, J. C., Isola, I., Regattieri, E. Coeval dry events in the central and eastern Mediterranean basin at 5.2 and 5.6 ka recorded in Corchia (Italy) and Soreq caves (Israel) speleothems. *Global Planetary Change* **2014**, *122*, 130 - 139. DOI: 10.1016/J.GLOPLACHA.2014.07.013
105. Drysdale R.N., Zanchetta, G., Hellstrom, J., Maas, R., Fallick, A., Pickett, M., Cartwright, I., Piccini, L. Late Holocene drought responsible for the collapse of Old World civilizations is recorded in an Italian cave flowstone. *Geology* **2006**, *34*, 101–104. DOI: 10.1130/G22103.1
106. Bar-Matthews, M. and Ayalon, A. Mid-Holocene climate variations revealed by high-resolution speleothem records from Soreq Cave, Israel and their correlation with cultural changes. *The Holocene* **2011**, *21*, 163–171. DOI: 10.1177/0959683610384165
107. Kaufman AJ, Wasserburg, G. J., Porcelli, D., Bar-Matthews, M., Ayalon, A., Halicz, L. U-Th isotope systematics from the Soreq cave, Israel and climatic correlations. *Earth and Planetary Science Letters* **1998**, *156*, 141–155. DOI: 10.1016/s0012-821x(98)00002-8.
108. Weyhenmeyer, C.E., Burns, S.J., Waber, H.N., Aeschbach-Hertig, W., Kipfer, R., Loosli, H.H., Matter, A. Cool Glacial Temperatures and Changes in Moisture Source Recorded in Oman Groundwaters. *Science* **2000**, *287*, 842–845. DOI:10.1126/science.287.5454.842.
109. Biasutti, M., Voigt, A., Boos, W.R., Braconnot, P., Hargreaves, J.C., Harrison, S.P., Kang, S.M., Mapes, B.E., Scheff, J., Schumacher, C., Sobel, A.H., Xie, S.-P. Global energetics and local physics as drivers of past, present and future monsoons. *Nature Geoscience* **2018**, *11*, 392–400. doi:10.1038/s41561-018-0137-1

110. Broccoli, A.J., Dahl, K.A., Stouffer, R.J. Response of the ITCZ to Northern Hemisphere cooling. *Geophysical Research Letters* **2006**, *33*, L01702. doi:10.1029/2005GL024546
111. Simon, M. H., Arthur, K., Hall., I. R., Peeters, F. J. C., Loveday, B. R., Barker, S., Ziegler, M., Zahn, R. Millennial-scale Agulhas Current variability and its implications for salt-leakage through the Indian-Atlantic Ocean Gateway. *Earth and Planetary Science Letters* **2013**, *383*, 101-112. DOI: 10.1016/j.epsl.2013.09.035
112. Gat J.R., Klein B., Kushnir Y., Roether W., Wernli H., Yam R. & Shemesh A. Isotope composition of air moisture over the Mediterranean Sea: an index of the air–sea interaction pattern. *Tellus Series B-Chemical & Physical Meteorology* **2003**, 55 (5), 953–965. DOI:10.3402/tellusb.v55i5.16395
113. Bowen, G.J. Spatial analysis of the intra-annual variation of precipitation isotope ratios and its climatological corollaries. *Journal of Geophysical Research: Atmospheres* **2008**, *113*, 1–10. doi:10.1029/2007JD009295
114. Gasse, F. Hydrological changes in the African tropics since the Last Glacial Maximum. *Quaternary Science Reviews* **2000**, *19*, 189–211. DOI: 10.1016/S0277-3791(99)00061-X
115. Johnson, T.C., Brown, E.T., McManus, J., Barry, S., Barker, P., Gasse, F. A High-Resolution Paleoclimate Record Spanning the Past 25,000 Years in Southern East Africa. *Science* **2002**, *296*, 113–132. DOI: 10.1126/science.10700571.
116. Lamb, H.F., Bates, C.R., Bryant, C.L., Davies, S.J., Huws, D.G., Marshall, M.H., Roberts, H.M. 150,000-year palaeoclimate record from northern Ethiopia supports early, multiple dispersals of modern humans from Africa. *Nature Scientific Reports* **2018**, *8*, 1077. DOI: 10.1038/s41598-018-19601-w.
117. Lyons, R.P., Scholz, C.A., Cohen, A.S., King, J.W., Brown, E.T., Ivory, S.J., Johnson, T.C., Deino, A.L., Reinthal, P.N., McGlue, M.M., Blome, M.W. Continuous 1.3-million-year record of East African hydroclimate, and implications for patterns of evolution and biodiversity. *Proceedings of the National Academy of Sciences* **2015**, *112*, 15568–15573. DOI:10.1073/pnas.1512864112.
118. Castañeda, I. S., J. P. Werne, and T. C. Johnson. Wet and arid phases in the southeast African tropics since the Last Glacial Maximum. *Geology* **2007**, *35(9)*, 823–826, DOI:10.1130/G23916A.1.
119. Schefuß, E., H. Kuhlmann, G. Mollenhauer, M. Prange, and J. Pätzol. Forcing of wet phases in southeast Africa over the past 17,000 years. *Nature* **2011**, *480(7378)*, 509–512, DOI:10.1038/nature10685.
120. Otto-Bliesner, B. L., J. M. Russell, P. U. Clark, Z. Liu, J. T. Overpeck, B. Konecky, P. deMenocal, S. E. Nicholson, F. He, and Z. Lu. Coherent changes of southeastern equatorial and northern African rainfall during the last deglaciation, *Science* **2014**, *346(6214)*, 1223–1227, DOI:10.1126/science.1259531.
121. Geyh, M.A., Heine, K. Several distinct wet periods since 420 ka in the Namib Desert inferred from U-series dates of speleothems. *Quaternary Research* **2014**, *81*, 381–391. DOI:10.1016/j.yqres.2013.10.020.
122. Pickering, R., Dirks, P.H.G.M., Jinnah, Z., de Ruiter, D.J., Churchill, S.E., Herries, A.I.R., Woodhead, J.D., Hellstrom, J.C., Berger, L.R. Australopithecus sediba at 1.977Ma and Implications for the Origins of the Genus Homo, *Science* **2011**, *333*, 1421-1423.
123. Voarintsoa, N.R.G., Brook, G.A., Liang, F., Marais, E., Hardt, B., Cheng, H., Edwards, R.L., Railsback, L.B. Stalagmite multi-proxy evidence of wet and dry intervals in northeastern Namibia: Linkage to latitudinal shifts of the Inter-Tropical Convergence Zone and changing solar activity from AD 1400 to 1950. *The Holocene* **2017c**, *27*, 384–396. DOI: 10.1177/0959683616660170.
124. Railsback, L.B., Brook, G.A., Liang, F., Voarintsoa, N.R.G., Cheng, H., Edwards, R.L. A multi-proxy climate record from a northwestern Botswana stalagmite suggesting wetness late in the Little Ice Age (1810–1820 CE) and drying thereafter in response to changing migration of the tropical rain belt or ITCZ. *Palaeogeography, Palaeoclimatolology, Palaeoecology* **2018**, *506*, 159–153. DOI:10.1016/j.palaeo.2018.06.029
125. Vogel, J.C., Kronfeld, J. Calibration of Radiocarbon Dates for the Late Pleistocene using U/Th Dates of Stalagmites. *Radiocarbon* **1997**, *39*, 27–32. DOI:10.1017/S003382220004087X.
126. Repinski, P., Holmgren, K., Lauritzen, S.-E., Lee-Thorp, J.A. A late Holocene climate record from a stalagmite, Cold Air Cave, Northern Province, South Africa. *Palaeogeography, Palaeoclimatology, Palaeoecology* **1999**, *150*, 269–277. DOI:10.1016/s0031-0182(98)00223-5
127. Holmgren, K., Karlén, W., Svanered, O., Lauritzen, S.-E., Lee-Thorp, J.A., Partridge, T.C., Piketh, S., Tyson, P.D. A 3000-year high-resolution stalagmite-based record of palaeoclimate for northeastern South Africa. *The Holocene* **1999**, *9*, 295–309. DOI:10.1191/095968399672625464
128. Stevenson, C., Lee-Thorp, J.A., Holmgren, K. A 3000-year isotopic record from a stalagmite in Cold Air Cave, Makapansgat Valley, Northern Province. *South African Journal of Science* **1999**, *95*, 46–48.

129. Cooke, H.J., Verhagen, B.T., 1977. The dating of cave development - an example from Botswana, in: Proceedings of the 7th International Speleological Congress Sheffield, England September 1977. pp. 122–124.
130. Cooke, H.J. The Palaeoclimatic Significance of Caves and Adjacent Landforms in Western Ngamiland, Botswana. *The Geographical Journal* **1975**, *141*, 430–444.
131. Shaw, P.A., Cooke, H.J. Geomorphic evidence for the late Quaternary palaeoclimates of the middle Kalahari of northern Botswana. *CATENA* **1986**, *13*, 349–359. DOI:10.1016/0341-8162(86)90009-3
132. Goslar, T., Hercman, H., Pazdur, A. Comparison of U-Series and Radiocarbon Dates of Speleothems. *Radiocarbon* **2000**, *42*, 403–414. doi:10.1017/S0033822200030332
133. Hennig, G.J., Grün, R., Brunnacker, K. Speleothems, travertines, and paleoclimates. *Quaternary Research* **1983**, *20*, 1–29. doi:10.1016/0033-5894(83)90063-7
134. Heine, K. On the ages of humid Late Quaternary phases in southern African arid areas (Namibia, Botswana). *Palaeoecology of Africa and the surrounding islands* **1992**, *23*, 149-164.